nanoenergy advances

MDPI

Review

Harvesting Wind Energy Based on Triboelectric Nanogenerators

Xuanyi Dong [1,2], Zhaoqi Liu [1,2], Peng Yang [1,2] and Xiangyu Chen [1,2,*]

[1] CAS Center for Excellence in Nanoscience, Beijing Institute of Nanoenergy and Nanosystems, Chinese Academy of Sciences, Beijing 100083, China
[2] School of Nanoscience and Technology, University of Chinese Academy of Sciences, Beijing 100049, China
* Correspondence: chenxiangyu@binn.cas.cn

Abstract: The utilization of various distributed energy is becoming a prominent research topic due to the rapid development of the Internet of Things and wireless condition monitoring systems. Among the various distributed energy sources, wind energy has the advantages of being widely distributed, renewable and pollution-free, and is a very promising mechanical energy for power supply. Traditional wind energy harvesting methods based on electromagnetic and piezoelectric effects have issues with complex structure, large size, severe mechanical structures, and high installation costs. The low frequency and irregular nature of ambient mechanical energy makes these methods generally inefficient and inevitably hinders the further exploitation of wind energy. The triboelectric nanogenerators (TENGs) based on frictional charging and electrostatic effects can also be used for wind power generation and are increasingly favored by researchers as TENGs are easier to be miniaturized and assembled, and can realize large-scale manufacturing in comparison. This paper reviews the research on TENGs for wind energy utilization in terms of structural design, material selection and potential applications. In addition, the potential difficulties and possible developments in this field are summarized and discussed.

Keywords: triboelectric nanogenerator; wind energy; energy harvesting

Citation: Dong, X.; Liu, Z.; Yang, P.; Chen, X. Harvesting Wind Energy Based on Triboelectric Nanogenerators. *Nanoenergy Adv.* **2022**, *2*, 245–268. https://doi.org/10.3390/nanoenergyadv2030013

Academic Editor: Joao Oliveira Ventura

Received: 19 July 2022
Accepted: 17 August 2022
Published: 22 August 2022

1. Introduction

Nowadays, adjusting the energy structure, alleviating environmental pollution and strengthening energy security have become the consensus of both academic and industrial world [1–3]. As one of the major branches of renewable energy, wind energy is a safe, renewable and extremely widely distributed green energy source. Wind power is now recognized as one of the most cost-effective ways to generate electricity. With the worldwide commitment to promote carbon-free power generation, wind power is becoming an increasingly important part of human daily life and is of great importance for the sustainable development of human society [4–6]. Traditional wind energy harvesting is mostly based on the electromagnetic induction principle and the piezoelectric principle. These devices often have high resistance ratios, are costly and their miniaturization can lead to significant cost increases and energy losses [7,8]. Therefore, it is essential to develop new, simple, geographically limited and cost-effective solutions for harvesting all forms of wind energy from the environment.

In 2012, Dr. Zhong Lin Wang proposed a new energy collection method—triboelectric nanogenerator (TENG), which can convert various mechanical energy into electricity based on the combination of electrostatic induction and contact electrification [9–11]. Due to its high energy conversion efficiency and large-scale manufacturing possibility, TENG is particularly suitable for the harvesting of irregularly distributed low mechanical frequency vibrational energy such as wind and ocean energy [12–14]. The concept of a wind-driven triboelectric nanogenerator (WD-TENG) has been developed to take advantages of the characteristics of wind energy and the high conversion efficiency of TENG. WD-TENG has been used in a variety of applications such as energy harvesting, potential alternative

energy sources for various portable electronic devices, wind vector sensors, and self-powered temperature and humidity sensors, significantly broadening the application range of TENG [15–17]. Meanwhile, there are many key points of WD-TENG, including the selection of materials and fabrication methods, common methods for performance optimization, cutting-edge applications and so on, have not been comprehensively summarized. Hence, a systematic review of the progress of WD-TENG is necessary for further promoting its development.

This paper describes the latest progress of WD-TENG. Firstly, the mechanism of WD-TENG for energy generation is discussed from the aspects of both mechanical design and electrification methods. Then, a series of crucial parameter that can decide the performance of WD-TENG have been thoroughly summarized, while the related performance optimization methods through structure design and material modification have also been elaborated with the consideration of different ranges of wind speed. The output characteristics of TENG and traditional wind energy device using electromagnetic generator (EMG) are compared, where the merits of each technique are carefully discussed. In addition, the combination of WD-TENG with other energy conversion mechanisms to realize the hybrid energy system for collecting energy from different sources is introduced, indicating tremendous application perspective in the field of distributed energy. Finally, based on these works, the existing problems as well as the important challenges of WD-TENG are proposed, in order to guide the future study of TENG for wind-related applications.

2. Energy Conversion Mechanism

In recent years, a lot of research based on TENG has been carried out in the field of wind energy collection. These experiments show that TENG has an edge over typical wind turbines in terms of energy conversion at low frequencies and low wind speeds. The power generating efficiency of TENG is substantially higher than standard wind turbines on the same volume scale [18,19]. TENG also has the advantages of a basic structure, a wide range of materials, a compact volume, low weight, and ease of production and installation. As a result, wind energy collection device installation is no longer limited to environments with high average wind speed and high wind energy density, such as open space and plains, but is increasingly being employed locally. TENG has four basic working modes: contact-separation (CS), lateral-sliding (LS), single-electrode (SE), freestanding (FT) to realize energy collection, and these four structures can realize the collection of wind energy under specific application conditions. Figure 1 clearly illustrates the common structural design and material selection of WD-TENG. TENG used for wind energy collection can be divided into “rotary type” [20–24] and “flow induced vibration type” [25–27] according to the way of energy collection. Among them, the working mode of rotating TENG is mostly independent layer type and sliding friction type and the “flow induced vibration type” is mostly vertical contact separation type.

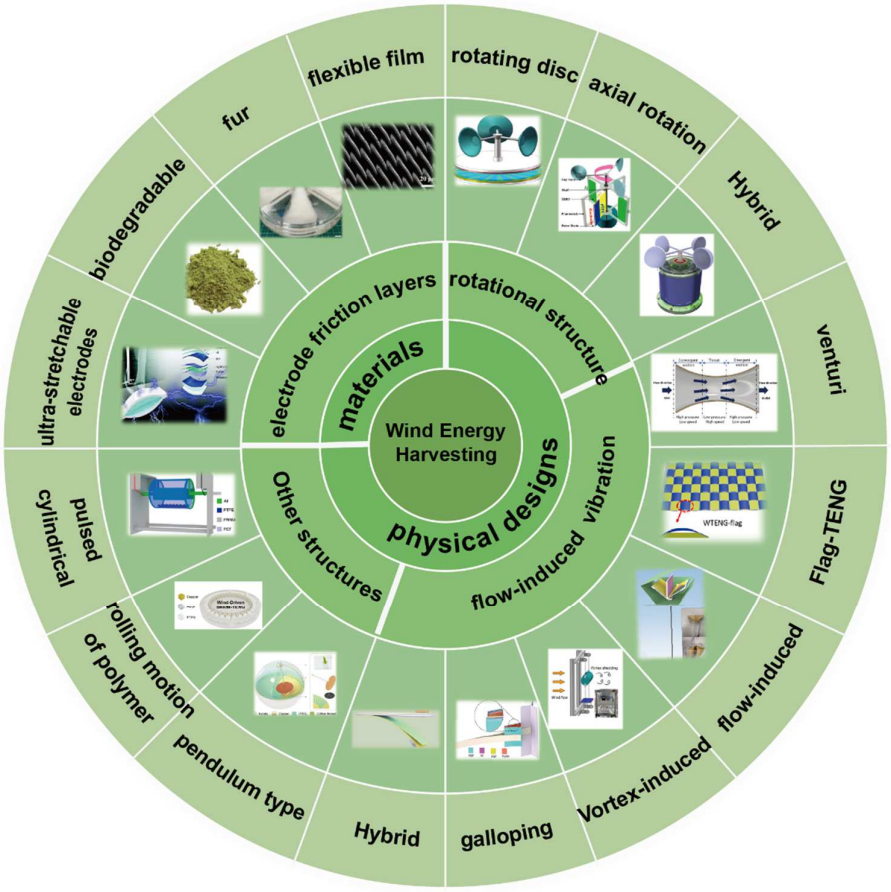

Figure 1. Overview of common materials and structures for WD-TENGs. Rotating disc. Reproduced with permission of [28], Copyright 2015, Nano Energy. Axial rotation. Reproduced with permission of [29], Copyright 2013, American Chemical Society. Hybrid rotation structure. Reproduced with permission of [30], Copyright 2018, Elsevier. Venturi system. Reproduced with permission of [31], Copyright 2019, Elsevier. Flag-TENG. Reproduced with permission of [32], Copyright 2016, American Chemical Society. Flow-induced WD-TENG. Reproduced with permission of [33], Copyright 2020, Elsevier. Vortex-induced WD-TENG. Reproduced with permission of [34], Copyright 2022, Elsevier. Galloping WD-TENG. Reproduced with permission of [35], Copyright 2020, Elsevier. Hybrid flow-induced WD-TENG. Reproduced with permission of [36], Copyright 2020, Springer. A pendulum type. Reproduced with permission of [37], Copyright 2019, Elsevier. WD-TENG based on rolling motion of beads. Reproduced with permission of [38], Copyright 2018, Elsevier. Pulsed WD-TENG. Reproduced with permission of [39], Copyright 2021, Elsevier. Ultra-stretchable electrodes. Reproduced with permission of [40], Copyright 2020, John Wiley and Sons. Biodegradable materials. Reproduced with permission of [41], Copyright 2019, Elsevier. Fur. Reproduced with permission of [42], Copyright 2021, John Wiley and Sons. Flexible film. Reproduced with permission of [43], Copyright 2021, Elsevier.

2.1. Material Electrification Mechanism

Triboelectrification is a common phenomenon in our life, and the discussion on the physical mechanism of contact electrification has never ended. In 2019, Wang et al. made a profound investigation into the mechanism of contact initiation on solid-solid surfaces, suggesting that electron transfer is the main mechanism of contact charging between solids and solids, and proposed the "electron cloud potential well" model to explain the contact initiation phenomenon between materials [44]. Friction electrification occurs in practically all materials we encounter in daily life, and the ability of different materials to gain and lose electrons varies. In 1957, John Carl Wilcke proposed a triboelectric sequence to characterize the polarity order of materials. The greater the distance between the two materials in

this process, the more electron gain and loss, and hence the more charge transferred. The surface topography of selected materials can be modified by micro-machining to improve the contact area and triboelectrification effect effectively [45–47]. The materials utilized to make WD-TENG must not only be widely apart in the triboelectric sequence, but they must also be resilient, durable, and cost-effective. Table 1 lists the classification, advantages and disadvantages of the materials commonly used in the production of WD-TENG.

Natural plants often have natural micro nano structures, which are biodegradable and easy to process, attracting more and more researchers' attention [48]. As shown in Figure 2a, Yang et al. designed a new leaf-based SE-TENG using Hosta leaf as electrode and friction material [49]. The smooth and compact upper surface of leaf can effectively reduce water evaporation, the pores on the back are used to ensure gas exchange, and the irregular surface structure can increase the effective contact area. However, the mechanical strength of natural leaves is not high, and its durability is poor with the continuous contact separation with other materials and the evaporation of water. In 2019, Feng et al. proposed a method of "crushing before reuse" and designed a wind-driven TENG with polyvinylidene fluoride (PVDF) and leaf powder as the friction layer [41]. Figure 2b shows the output performance of TENG made of fresh leaf and dry leaf powder. It can be seen that the output of leaf powder based TENG (LP-TENG) is better, and the free water in fresh leaves reduces the generation of electrons. In order to further improve the output performance of LP-TENG, the chemical modifiers called Poly-L-Lysine(PLL) were used to change the surface characteristics of the blade, which can effectively improve the output performance of TENG. In 2021, Han et al. selected the low-speed electric friction layer as a kind of friction material for the rotary electric generator, illustrated in Figure 2c [42]. Rabbit hair has the characteristics of softness and good elasticity. When in close contact with another friction layer material, the friction resistance is small. While reducing the starting wind speed, it improves the durability of the equipment. When the wind speed is 6 m/s, its instantaneous peak power can reach 11.9 mW.

Table 1. Summary and comparison of frequently used tribo-active materials for WD-TENG.

Classification	Categories	Advantages	Disadvantages
Metals and its derivatives	Metal, alloy, semiconductor metallic nanoflakes/nanoparticles/nanowires	Excellent electrical conductivity, high stability, high mechanical robustness, simple process	Low flexibility
Conducting polymers	PTFE, PVDF, PDMS, PMMA	Easy structural control, heat resistance, corrosion resistance, light weight, good flexibility	Relatively high cost, poor conductivity, low stability, Non-biodegradable, Not-recyclable
Carbonaceous fillers	Graphite, CNT, Graphdiyne	High conductivity, high stability, good mechanical properties	Cumbersome processing technology
Natural materials	Rabbit Fur, leaves	Flexible, low cost, biodegradable and easy to process	Poor electrical conductivity, poor durability
Composite materials	Combination of different conductive materials (e.g., graphene-PDMS)	Synergistic effect	Increased preparation cost and workload

As displayed in Figure 2d, Li et al. fabricated a self-powered wind speed sensor with superhydrophobic properties using methyl-graphdiyne (M-GDY) [50]. Stable arrays of superhydrophobic M-GDY nano thorn arrays were constructed on copper substrates using a wet chemical method. A new type of wind speed sensor with water and cold resistance

was developed by using the new methyl substituted GDY nano thorn array as electrode. In 2020, as can be seen from Figure 2e, Ren et al. used an ultra-thin Ecoflex as the wind energy capture unit and attached thermoplastic polyurethane (TPU) fibers doped with ultra-long silver nanowires (AgNWs) on the upper and lower surfaces of the film as the friction electrode [40], and the Al electrode and the FEP film were attached to the upper and lower inner walls of the arched frame, respectively. The lighter mass of the electrode and the microporous structure introduced on it effectively enhance the vibration performance of the electrode and make it easy to work under breeze drive. The device achieves an average power density of 20 mW/m^3 at 0.7 m/s, which greatly reduces the threshold wind speed.

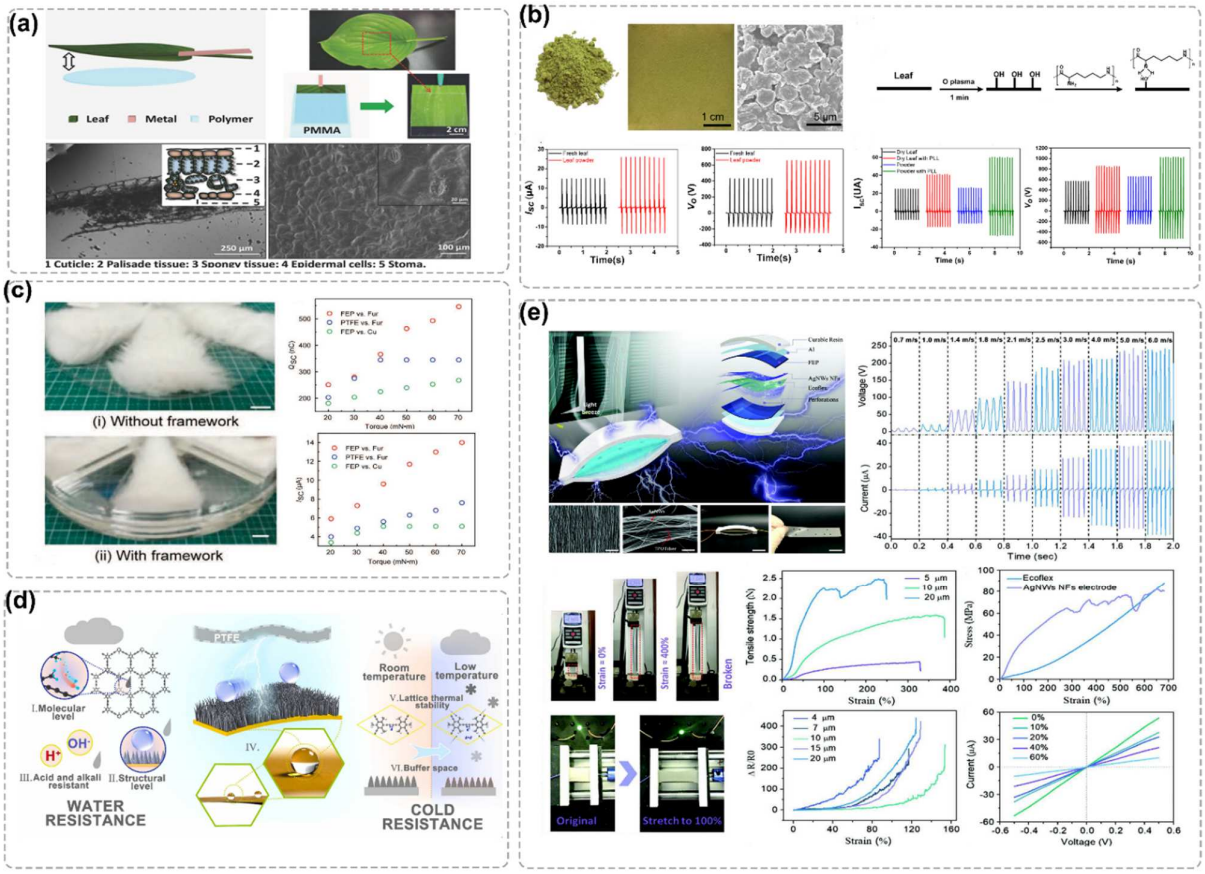

Figure 2. Typical materials of WD-TENG. (**a**) Natural plant leaves as friction layer. Reproduced with permission of [49], Copyright 2018, John Wiley and Sons. (**b**) The leaf powder-based TENG. Reproduced with permission of [41], Copyright 2019, Elsevier. (**c**) Rabbit fur as friction layer. Reproduced with permission of [42], Copyright 2021, John Wiley and Sons. (**d**) Schematic diagram of M-GDY resisting water interference during power generation. Reproduced with permission of [50], Copyright 2021, Elsevier. (**e**) The unidirectional TPU spinning NFs modified by ultra-long AgNWs. Reproduced with permission of [40], Copyright 2020, John Wiley and Sons.

2.2. Utilization Mechanism of Mechanical Energy

2.2.1. Wind-Induced Rotation

The structural design of rotating wind energy collection TENG is mainly inspired by the traditional electromagnetic wind turbine, with the help of wind cup or other structures to collect wind energy, and convert it into rotating mechanical energy to drive the contact separation of TENG friction layer, so as to produce electrical output. Wind energy collection devices based on rotating structure usually have dense peak output and high output power, mostly in the form of separate layers and rotating slides.

The typical rotary-disk slip structure is shown in the Figure 3a,b [28]. Its basic structure is composed of wind cup, rotor and stator. Driven by the wind, the wind cup drives the

rotor to rotate. The key parts of the stator and rotor are radial upper and lower grating Cu electrodes made by printed circuit board (PCB) technology. Among them, the bottom electrode is composed of two groups of complementary electrodes with a layer of Kapton film on it. When the external wind acts on the WD-TENG, the Cu electrode of the rotor part slides relative to the Kapton film, resulting in electric output. The most obvious feature of sliding translation mode is that the interaction area is large, which effectively ensures its output performance. Using this structure, a simple self-powered air cleaning system is designed.

Compared with the typical rotary-disk structure, the axial rotary structure saves more space [20,29,51]. When the friction area is the same, the horizontal scale occupied by the cylindrical TENG is smaller. As shown in Figure 3c, its working mode is a mixed process of contact-sliding-separation-contact process, which innovatively combines two basic modes. When the wind blows to the wind cup, the wind cup will drive the rotor blades to rotate around the shaft. At first, the polytetrafluoroethylene (PTFE) film contacted completely the aluminum of either stator, and then with the bending of the polyethylene terephthalate (PET) part, the PTFE film will slide outward on the aluminum surface. With the continuous and alternating progress of this process, electrical output is generated. When the wind speed is 15 m/s, the R-TENG generates an open circuit voltage of 250 V and a short circuit current of 0.25 mA. The maximum power is 62.5 mW. It can directly light hundreds of commercial LEDs or effectively charge energy storage units.

The wind energy acquisition system based on rotating structure is often simple in structure, and its output performance can be improved through full contact between friction layers. However, the accompanying friction heat and material wear will seriously damage the electrical stability and mechanical durability of TENG, increase its rotation resistance and high starting wind speed. Moreover, the conversion mechanism of this structure itself corresponds to large energy loss. Researchers often use material modification, structural breakthrough or combination with other energy conversion mechanisms such as EMG to reduce the starting wind speed and improve the output performance, so as to continuously realize the reliability and practicability of the structure.

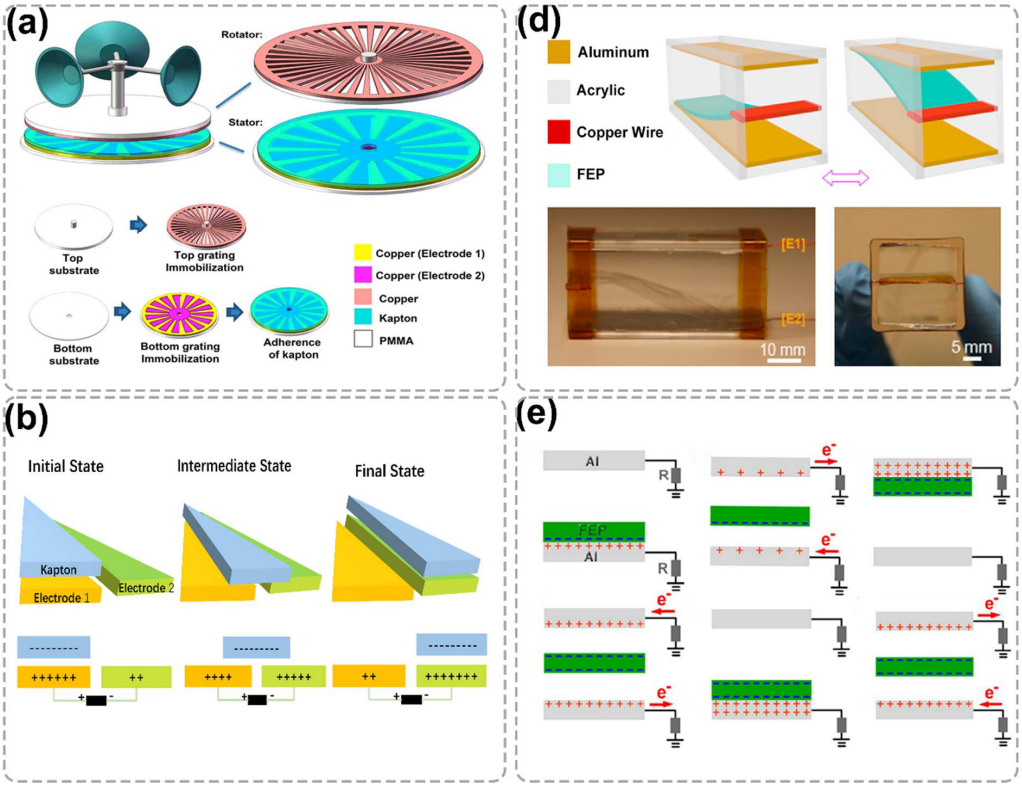

Figure 3. *Cont.*

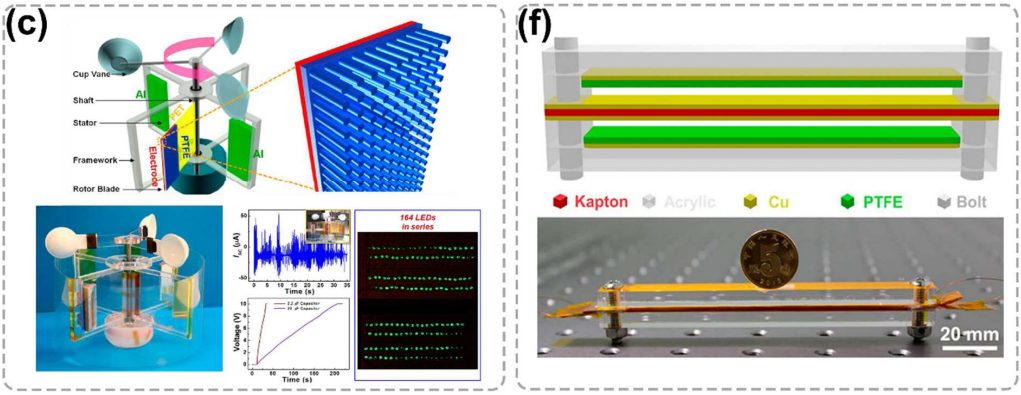

Figure 3. Typical structure and mechanism of WD-TENG. (**a**) In-plane cycled sliding mode of WD-TENG. Reproduced with permission of [28], Copyright 2015, Elsevier. (**b**) Working mechanism of rotary WD-TENG. (**c**) Rotational sweeping mode of WD-TENG. Reproduced with permission of [29], Copyright 2013, American Chemical Society. (**d**) Single-side-fixed mode of WD-TENG. (**e**) Working mechanism of flutter-driven WD-TENG. Reproduced with permission of [52], Copyright 2013, American Chemical Society. (**f**) Double-side-fixed mode of WD-TENG. Reproduced with permission of [53], Copyright 2015, American Chemical Society.

2.2.2. Flow-Induced Vibration

Although rotary wind energy collection can effectively realize wind power generation, such devices must first convert wind energy into rotary kinetic energy before driving TENG to work. There is a large energy loss in this process. As a result, scientists prefer to convert the flowing wind energy directly into the device's vibration energy, which is why the flow-induced TENG was invented [54]. In order to realize the effective utilization of distributed energy, the energy collection structure is becoming more and more miniaturized and integrated, and more attention is paid to the collection of breeze energy and its achievable effective wind speed range. Based on these needs, the advantages of flow-induced vibration wind energy collection device are becoming more and more obvious.

Yang et al. first reported TENG driven by fluorinated ethylene propylene (FEP) film's flutter, as shown in the Figure 3d [52]. The TENG structure is composed of a rectangular acrylic frame, two pieces of aluminum (Al) foils and FEP film with nanowires on the surface. One side of the FEP membrane is fixed and the other side remains independently suspended. Driven by the external wind, the FEP membrane vibrates in the direction perpendicular to the air flow, and periodic contact separation will occur between the upper and lower electrodes, driving electrons to flow back and forth between the electrodes and the ground to produce electrical output. When the size is 2.5 cm × 2.5 cm × 22 cm, the output voltage of the structure is up to 100 V and the output current is 1.6 μA. When the external load is 100 MΩ, the output power is 0.16 mW, which can be used to directly light dozens of commercial light-emitting diodes.

This theoretical model of the contact separation mode is shown in Figure 3e: in the initial state, the FEP film is in complete contact with the lower electrode. Due to the different electronic affinity of materials, the surfaces of Al and FEP have positive and negative friction charges, respectively. Driven by the external wind, the FEP film is separated from the bottom electrode, and the FEP will drive the free electrons to flow to the external circuit. At this time, in the external circuit, the electron movement directions of the top and bottom Al electrodes are opposite. Until the negative friction charge of FEP film completely shields the total positive charge, the external circuit will no longer show current. When the FEP film contacts the upper electrode, all induced charges are attracted to the upper electrode. The electrons flow from the ground to the upper electrode as FEP gradually moves away from the higher electrode. At the same time, the gap between FEP and the bottom Al electrode shrinks, allowing electrons to flow from the bottom Al electrode to the ground until they make complete contact with the lower electrode. All

induced charges are attracted to the lower electrode, and there is no electron flow in the external circuit. TENG causes electrons to bounce between the Al electrode and the ground, generating alternating current in the external circuit.

The output electrical signal of unilateral fixed WD-TENG is not particularly stable due to the arbitrary swing of independent film. In 2015, Wang et al. reported a WD-TENG driven by elastic aerodynamics, as shown in the Figure 3f [53]. Both the upper and lower substrates use Cu as electrode and PTFE as triboelectric layer. The Kapton film with Cu electrodes attached at the top and bottom is fixed in the center of the equipment through two bolts. The whole structure is composed of two TENGs. Between the PTFE and Kapton films, two thin air gaps are generated. The air fluid is loaded into the above gap and vibrates the Kapton film, resulting in the contact and separation of Cu and PTFE film, resulting in electrical output.

3. Structural Display of WD-TENG

3.1. Design Based on Rotational WD-TENG

Most of the TENGs used to convert rotating mechanical energy in the environment into electrical energy are based on sliding or free-standing layers. The working mechanism of these structures will bring about severe wear of the frictional electrical layer and the TENG will have to overcome the corresponding frictional resistance to work, resulting in reduced output performance, higher starting wind speeds and reduced working life and high maintenance costs. Of the four basic modes of TENG, the FT-TENG is more tolerant of the distance between friction layers and therefore supports power generation in non-contact mode. In 2015, Li et al. proposed an independent layer-based operating mode that can automatically switch between contact and non-contact, as depicted in Figure 4a [55]. The effect of contact and non-contact on the output performance of rotating TENGs was investigated. This new design can significantly reduce surface wear and maintain a high output by replenishing the frictional charge in the contact state. As illustrated in Figure 4b, Li et al. demonstrated that a lightweight rotor could reduce the kinetic energy changes caused by unstable wind conditions by selecting a low-density material for the rotor and investigating the effect of rotor mass on the energy conversion rate at different speeds [56]. With the aid of a suitable wind cup structure, this rotating TENG can effectively reduce the starting wind speed to 3.3 m/s while reducing friction losses, allowing for effective breeze energy harvesting. At a wind speed of 4 m/s, the energy conversion efficiency is up to 12.06%. Yong et al. have designed a dual-axis TENG based on the integration of two coaxial TENGs with different geometrical parameters, as can be seen from Figure 4c, which complement each other's performance by optimizing the dimensions of the two independent TENGs and the wind cup arm length [57]. The start-up wind speed can be as low as 2 m/s and has a wide range of collection wind speeds.

3.2. Design Based on Wind-Induced Vibration Mode

Flow-excited vibrations offer significant advantages in the field of miniaturization, integrated wind energy harvesting devices and the harvesting of breeze energy. Four flow-induced vibration phenomena are generally used to convert fluid energy into mechanical kinetic energy: vortex vibration, galloping, flutter and wake-galloping. Based on these theories, researchers have been constantly updating their structures to improve the efficient use of wind energy in recent years.

In 2013, Bae et al. designed a flutter-driven triboelectric generator (FTEG) based on the interaction of a flexible flag fabric arranged in parallel with a solid plate [58]. Under the action of wind, the flexible flag with metal attached to its surface undergoes self-sustaining oscillations and is continuously separated from the rigid plate by contact-like contact, resulting in electrical output. At a wind speed of 15 m/s, an average power of 0.86 mW can be achieved. In 2016, Su et al. developed a novel thin-film-based segmented triboelectric nanogenerator (S-TENG) [59]. This segmented structure can effectively suppress the internal cancellation caused by changes in oscillating film potential. Each segment has a pair

of electrodes and can be regarded as a small TENG operating independently. Comparative measurements were carried out through each cell, integrated segmented device and non-segmented device. The results show that the amplitude of the total output current of the segmented S-TENG is significantly greater than that of the non-segmented S-TENG, indicating that the segmented electrode structure effectively reduces the cancellation effect. At a wind speed of 17.9 m/s, the segmented S-TENG has an open circuit voltage of up to 36 V and a short circuit current of 11.8, corresponding to a maximum output power of 114.7 uW.

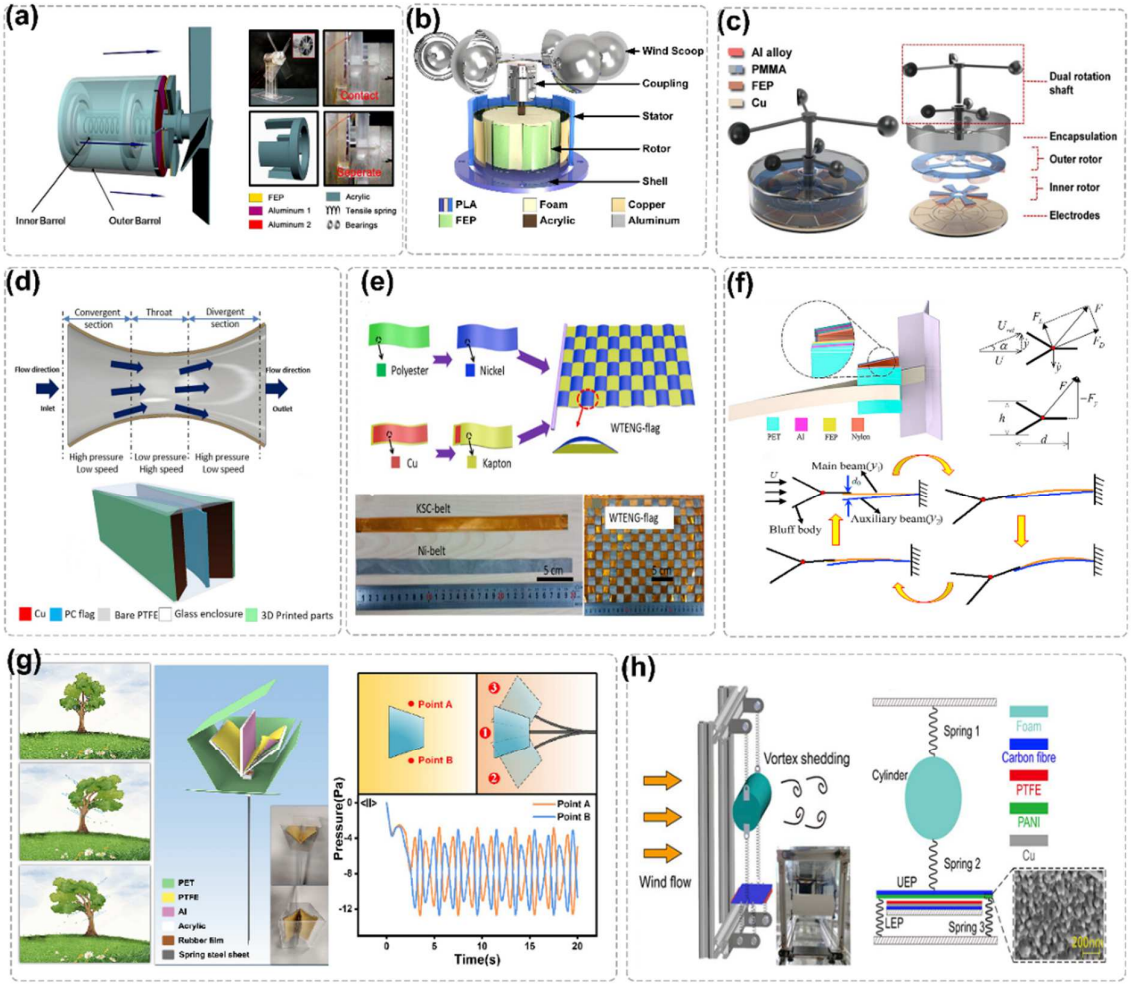

Figure 4. Various structures of WD-TENG: (**a**–**c**) Rotary structures. (**a**) WD-TENG switching between contact and non-contact modes. Reproduced with permission of [55], Copyright 2015, American Chemical Society. (**b**) Rotary WD-TENG with lightweight rotor. Reproduced with permission of [56], Copyright 2021, Elsevier. (**c**) A dual-rotation shaft WD-TENG. Reproduced with permission of [57], Copyright 2021, John Wiley and Sons. (**d**–**f**) Structures based on flow-induced vibration. (**d**) TENG based on wind actuated venturi design. Reproduced with permission of [31], Copyright 2019, Elsevier. (**e**) Woven WD-TENG flag. Reproduced with permission of [32], Copyright 2016, American Chemical Society. (**f**) WD-TENG based on galloping response. Reproduced with permission of [35], Copyright 2020, Elsevier. (**g**) WD-TENG based on cantilever beam structure. Reproduced with permission of [33], Copyright 2020, Elsevier. (**h**) Vortex-induced vibration based WD-TENG. Reproduced with permission of [34], Copyright 2022, Elsevier.

For the WD-TENG with parallel structures fixed on both sides. In 2014, Seol et al. sufficiently reduced the device thickness by sharing interlayer electrodes [60]. The researchers further investigated the performance improvement due to the disposed stacked structure, and as a result, an increase in output power was achieved. The vertically stacked

triboelectric nanogenerator (VS-TENG) achieves an efficient use of natural wind in both wind directions. However, similar parallel-structured TENGs often suffer from insufficient friction layer contact and their output performance is optimized by the gap between the parallel plates, requiring complex structural design. In 2019, Lin et al. proposed an angle-shaped TENG (AS-TENG) based on an independent frictional electric layer operating mode [61]. The device consists of two Al layers stacked to form an angular shape, and the two Al layers share the frictional electric layer FEP film located between them. The FEP film can be in full contact with the Al layers. The AS-TENG introduces a wedge-shaped wind guide channel on the windward side, which significantly reduces the start-up wind speed. It has been verified experimentally: the rectified ISC (2.5 μA) and V_{OC} (64 V) of the angled structure can be more than three times larger than that of the parallel structure. Furthermore, taking advantage of the angled structure, the manufactured TENG can be easily integrated by connecting each unit back-to-back and sharing a common vertex. By connecting them in parallel, the total electrical output can be increased exponentially. In 2019, a state-of-the-art TENG based on wind actuated venturi design system is demonstrated in sync with the smart system evolution for powering various sensor nodal network. As shown in Figure 4d [31], the system consists of three main parts: inlet, outlet and throat. As ambient air passes through the Venturi system, there is a low pressure in the throat region that forces the flag membrane to flutter at a high frequency between the electrodes. With increase in wind velocity, the throat pressure decreases, increasing the flag fluttering frequency. By adjusting the incoming wind speed and optimizing the gap distance of the structure, the structure can generate a peak power of 4.5 mW, an output performance that exceeds all previous work and demonstrates the feasibility of the structure in the field of wind energy harvesting.

The flutter-driven TENGs described above are usually confined to a gas tube and are generated by the interaction of a thin film with a rigid plate. This structure is bulky and limits the ability of the TENG to collect wind energy in different directions. In 2015, Zhao et al. investigated a lightweight, freestanding woven-flag type frictional electric nanogenerator (WTENG-flag) [32]. As shown in Figure 4e, nickel strip electrodes are made by chemically coating the upper and lower surfaces of a commercially available flexible polyester fabric with nickel film and Kapton film-sandwiched Cu belts (KSC belts) are obtained by sealing the sides of the copper foil with Kapton film (20 μm thick). The WTENG is formed by interweaving the top and bottom sandwich structures. The output performance is optimized by optimizing the dimensions and the tightness between the two bands. By stacking this 2D form of the WTENG-flag in parallel, an almost linear increase in output is obtained. The adaptability of this 2D WTENG-flag to different environments, especially at low temperatures and low humidity at high altitudes, was also verified. The flag-type TENG designed above is not flexible in the practical sense, as the electrodes corresponding to its flexible membrane are rigid and fixed. In 2016, Zhang et al. designed strip-like TENG units with several individual polymer arrays arranged vertically to make a lawn-like arrangement to capture energy in natural wind [62]. In 2020, Wang et al. proposed a moisture-resistant, wind-adapted TENG [63]. The study encapsulated the electrodes and PTFE membrane in PET. The frictional electric layer was isolated from air to prevent water-vapor adsorption on the PTFE surface and to avoid its power generation performance being affected by the relative humidity of the air. The experimental results show that there is no significant difference in the output performance under different relative humidity conditions. The flag type TENG can be used as a sensor for measuring wind speed and indicating wind direction, and can achieve effective wind energy harvesting under humid conditions. In 2020, the Sun et al. team designed a fluttering double-flag type triboelectric nanogenerator (FD-TENG) for ambient wind energy harvesting, a fully flexible flag-type TENG that is more prone to chattering at low wind speeds [64]. The output power density can reach 600 mw/m^2 when the wind speed is 10 m/s. The Flag-TENG based on thin film flutter has excellent energy harvesting performance at higher wind speeds.

In the above literature, the wind speed that can effectively drive these TENGs is typically above 5 m/s, while the global average land wind speed near the surface (observed at 10 m) is 3.28 m/s [65]. The low efficiency at low wind speeds in some degree limits the application of these TENG devices in the general environment. In 2020, Zhang et al. designed a galloping structure to harvest wind energy, as shown in Figure 4f [35]. The structure consists of a main beam, a secondary beam and a blunt body attached to the free end of the main beam. Based on the galloping response of the main beam, contact separation occurs between the two films, nylon and FEP, resulting in a continuous AC voltage. The researchers discuss the conditions of the fluid forces that trigger the chordal motion. The researchers studied the contact separation and output performance between primary and secondary beams with different length configurations. The two different modes of operation are single contact and double contact when using different length configurations of main and secondary beams. The single contact mode of the galloping triboelectric nanogenerator (GTENG) showed a greater electrical output at low wind speeds. We demonstrate a self-supporting GTENG in a 12 × 9 configuration generating a peak voltage of 200 V at a wind speed of 1.4 m/s using a 3 cm × 3 cm frictional electrical film. Zeng et al. designed a wind energy harvesting TENG based on a cantilever beam structure supporting a cylindrical bluff body, the energy capturing body of which is a trapezoidal column supported by a spring steel sheet in which two back-to-back contact separated forms of TENG are placed, as depicted in Figure 4g [33]. This design separates the TENG part from the wind drive component, avoiding environmental disturbances and reducing unnecessary frictional wear. When the air flow passes over the surface of the bluff body, the pressure loads on both sides of the trapezoidal section alternately reaches the amplitude, and the whole system oscillates reciprocally with the fixed end of the spring steel piece as the origin, thus driving the TENG electrode encapsulated in the bluff body to contact and separate, thus realizing the conversion of wind energy–kinetic energy of bluff body–kinetic energy of TENG–electrical energy. This innovative design provides a new way of efficiently collecting wind energy from light to moderate gusts. In 2021, Zhang et al. elucidated the theoretical model of the VIV-TENG engine and proposed a novel vortex-excited vibrating frictional electric nanogenerator (VIV-TENG), as depicted in Figure 4h [34]. Its structure is shown in Figure 4h. Driven by the lateral wind, the light cylinder undergoes vortex vibration, causing periodic contact separation of the polyaniline (PANI) and PTFE films as friction layers to generate electrical output. The VIV-TENG has a higher average output power than most previous studies and has a lower starting wind speed. Further, to overcome the narrow locking region, two cylinders were placed in series to obtain the T-VIV-TENG with a broadband resonant wind speed between 2 and 7 m/s, achieving a high output power over a wide range of wind speeds.

3.3. Other Structures

In addition to the common structures mentioned above, special structures have been designed to achieve efficient wind speed harvesting [66]. In 2018, Kim et al. proposed a WD-TENG that uses polymer micro-beads and their sliding motion in a novel structure to capture the mechanical energy of the wind drive, as shown in Figure 5a [38]. The open circuit voltage and short circuit current can reach 18.5 V and 2.3 μa, respectively, at wind speeds of 10 m/s. The structure enables wind energy to be collected in any direction and the electrical output performance changes rapidly and proportionally with wind speed, allowing it to be used as a self-powered wind speed sensor. Due to the relative flatness of the device, it is easy to integrate. When it is made in a stacked form, its output performance can be further improved.

In 2019, inspired by the pendulum structure, Lin et al. designed a symmetrical pendulum-based structure TENG, as shown in Figure 5b [37]. In order to increase the vibration level combined with a reduction in friction, a separate gap of 1 mm is left between the pendulum triboelectric layer and the electrode layer. The pendulum triboelectric layer is connected to the external acrylic spherical shell by means of a cotton thread for free

vibration. This structure is very sensitive to external vibrations and small disturbances can cause large oscillations in the pendulum friction layer. The researchers compared the output performance of the pendulum inspired TENG (P-TENG) with that of an in-plane TENG and found that it is 14.2 times more capable of acting as a sustainable energy source than a conventional freestanding TENG, demonstrating its superior energy harvesting capability.

The rotary FS-TENG stands out among the various energy harvesters/generators due to its intensive peak output and high output power. However, it usually requires various rotational motions to drive it, which hinders its use in the prevalent exploitation of low frequency vibrations and linear motions. A series of studies were performed to convert rotational motion into linear motion to trigger TENG work [23,67,68]. As exhibited in Figure 5d, Lu et al. designed a bidirectional gear transmission triboelectric nanogenerator (BGT-TENG). Under the action of an external excitation, the plate undergoes a reciprocating motion, which transmits mechanical energy via the rack to the two reverse-mounted gear trains and further triggers the continuous rotation of the flywheel. By connecting it to a rectifier bridge, an effective power supply for commercial thermometers was achieved, showing its potential application in the field of energy harvesting.

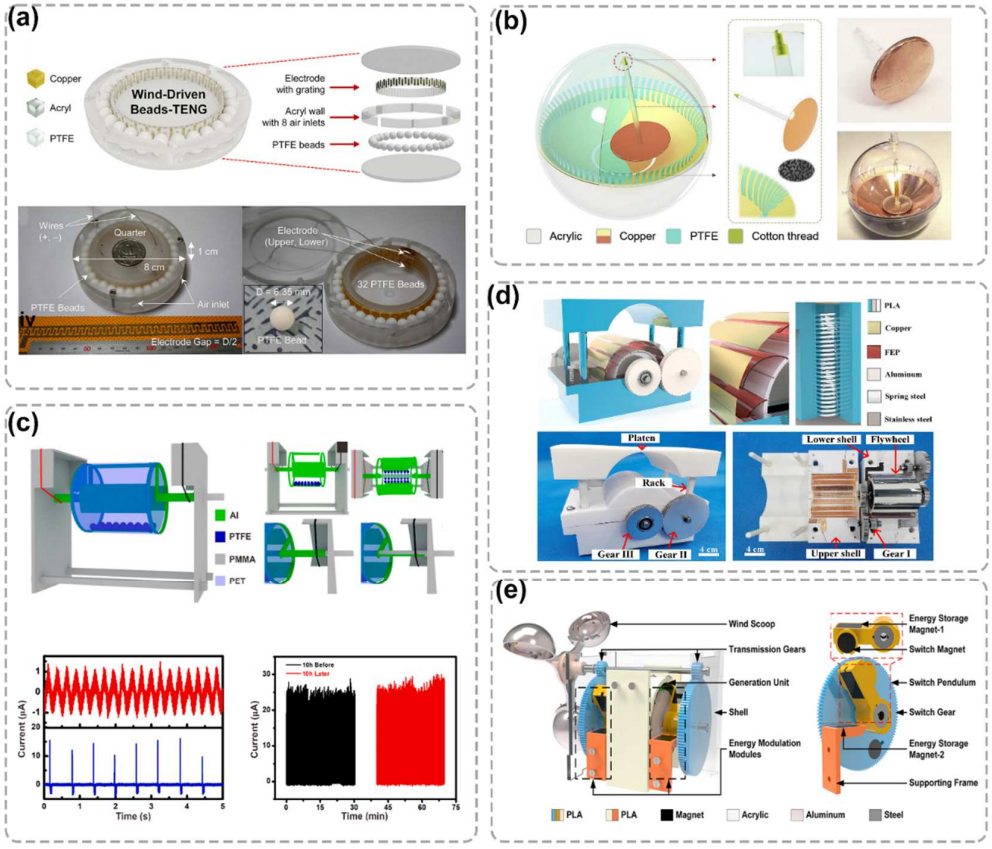

Figure 5. Other structures of WD-TENG. (**a**) WD-TENG based on rolling motion of beads. Reproduced with permission of [38], Copyright 2018, Elsevier. (**b**) A pendulum-spired WD-TENG. Reproduced with permission of [37], Copyright 2019, Elsevier. (**c**) A pulsed cylindrical WD-TENG. Reproduced with permission of [39], Copyright 2021, Elsevier. (**d**) A bidirectional gear transmission triboelectric nanogenerator (BGT-TENG). Reproduced with permission of [23], Copyright 2020, Elsevier. (**e**) WD-TENG controlled energy collection by magnetic switch. Reproduced with permission of [69], Copyright 2021, Elsevier.

In Figure 5c, a novel free-standing layer TENG structure based on the contact separation of PTFE particles and Al electrodes was proposed, creatively using a real-time signal output terminal structure (RTS) and the pulsed signal output terminal structure

(PTS) to characterize the output performance of the TENG [39]. Experiments show that the current at the pulsed signal output can reach more than 13 times that at the real time signal output with better stability, demonstrating the advantages of the pulsed TENG for energy harvesting, which can capture low frequency mechanical energy from wind and water. Low cost, high efficiency conversion of electrical energy to drive the electrolysis of hydrogen in seawater.

In order to provide continuous, regular electrical energy above a critical speed, as can be seen from Figure 5e, Liu et al. designed a magnetic switch structured triboelectric nanogenerator (MS-TENG) consisting of a drive gear, an energy modulation module and a power generation unit with a magnetic switch structure [69]. Unlike previous designs, the storage and release of energy from this structure is determined by the magnetic force of the magnet and does not depend on the wind speed. The MS-TENG supplies 500 LEDs in series and a thermometer, showing that the MS-TENG has good prospects for wind energy harvesting applications. Its design advantages in converting wind energy into a reliable electrical output could provide a useful guide for future wind energy harvesting.

4. Applications of WD-TENG

As the designs of WD-TENG become smaller, lighter, and more durable, they become more adaptable to varying wind speeds, humidity, and other external environmental conditions [70]. WD-TENG shows great potential in various applications such as powering small electronic devices, as secondary energy stored in capacitors, as self-powered sensors for wind vectors or parameters such as humidity, and self-powered electrochemical systems, as depicted in Figure 6a–f.

The interaction of flexible flags with steel plates as a powerful vibration source for triboelectric nanogenerator has attracted extensive attention from researchers. In 2017, Xu et al. designed a TENG based on aeroelastic flutter-based TENG (AF-TENG) and investigated different chattering behaviors caused by differences in the size, liquid-solid mass ratio, and bending stiffness of the flexible film, and actively sensed the wind speed by measuring the flutter frequency [71]. In 2018, Liu et al. reported for the first time a system capable of polarizing $BaTiO_3$ (BTO) materials, making full use of the high voltage and low current characteristics of TENG [69]. By comparing the effectiveness of commercial DC polarization equipment (DC-PE) and TENG for polarizing ferroelectric BTO films with thicknesses between 0.3 mm and 0.7 mm, it was found that higher piezoelectric and pyroelectric constants were obtained for most samples polarized with TENG polarization.

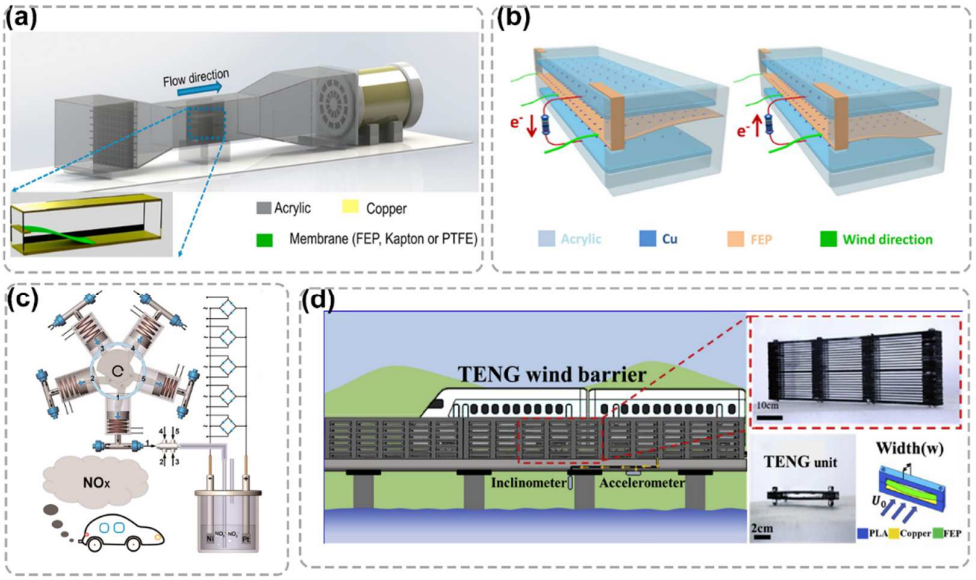

Figure 6. *Cont.*

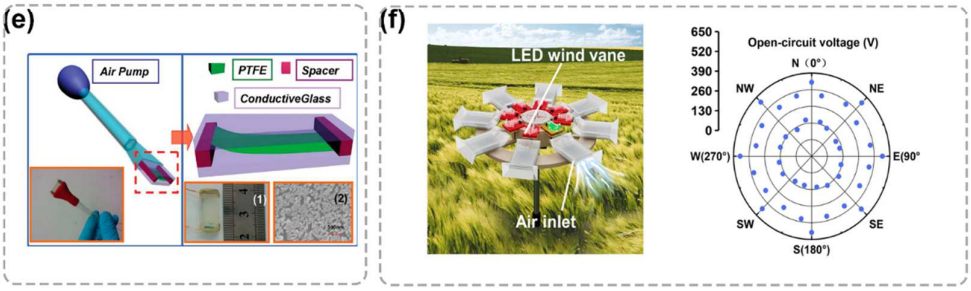

Figure 6. Applications of WD-TENG. (**a**) Experimental set-up and characterization of fluttering behavior of AF-TENG. Reproduced with permission of [71], Copyright 2017, Elsevier. (**b**) Schematic diagram and working mechanism of ferroelectric BTO disk polarized by WD-TENG. Reproduced with permission of [72], Copyright 2017, Elsevier. (**c**) Self-powered air purification system. Reproduced with permission of [73], Copyright 2020, ACS Nano. (**d**) Application scenario of the TENG-based wind barrier. Reproduced with permission of [16], Copyright 2020, Nano Energy. (**e**) Schematic diagram and (inset) digital photograph of the designed ATNG sensor. Reproduced with permission of [74], Copyright 2014, American Chemical Society. (**f**) WD-TENG is used to realize self-powered wind vector monitoring. Reproduced with permission of [75], Copyright 2021, Elsevier.

In 2019, Han et al. designed a self-powered NO_X uptake and nitrate and nitrite degradation system driven by wind energy [73]. This program is characterized by low cost, simple equipment and easy availability of materials. This work provides a basis for future applications in the field of pollutant gas removal in the TENG environment. In 2020, Liu et al. designed an efficient wind barrier based on WD-TENG to collect natural wind and slipstream energy induced by vehicle travel. Self-driven wind speed sensing can also be performed using the flutter frequency of the film. Guo et al. designed a self-powered humidity sensor by taking advantage of PTFE' s sensitivity to dielectric constant, which can simultaneously detect humidity and airflow velocity [74]. In 2022, Dai et al. prepared an omnidirectional wind energy harvester (OWEH) consisting of eight slit-effect based frictional electric nanogenerators (TENG) using transparent degradable hydroxyethyl cellulose (HEC) films, as shown in Figure 6f, for wind energy harvesting and self-supplied wind vector monitoring. By analyzing the eight independent output signals in real time, wind speed information can be obtained with a wind speed sensitivity of 78.36 V/(m/s). LED lights indicate the wind direction at this time. This work provides new ideas for further intelligent agriculture.

5. WD-TENG Hybridized with Other Types of Generators

In order to realize the complementary advantages of various energy conversion mechanisms in obtaining mechanical energy and self-powered sensing, the combination of TENGs with electromagnetic and piezoelectric energy collection mechanisms is considered. Let us start with the mixture of multiple mechanisms. In 2018, Qian et al. designed a wind hybrid energy harvester (WH-EH) consisting of a TENG, two EMG groups and solar cells [30], as shown in Figure 7a. The WH-EH is demonstrated to light hundreds of LEDs and power small electronics. This research further advances solid progress in the practical application of hybrid nanogenerators for mechanical energy harvesting and self-powered wireless sensor monitoring systems.

As exhibited in Figure 7b, Zheng et al. developed a hybrid generator based on TENG and pyroelectric-piezoelectric nanogenerators (PPENGS) that can harvest wind and thermal energy separately or simultaneously [76]. In this case, the wind-driven TENG is based on a chattering structure that uses PVDF film at the bottom to create a PPRNG for thermal energy harvesting. When the PPENG is hybridized with the TENG, the charging rate of a 22 μF capacitor is increased by a factor of almost three. Integration of this structure into a mask to capture energy through human breathing has been used in the field of medical monitoring. Rahman et al. integrated three energy harvesting units, TENG, PENG and EMG, into a

rotating system to form a fully enclosed wind turbine, as shown in Figure 7c [77]. The flexible piezoelectric layer PVDF with PET substrate is attached to the wind-driven rotating system as a PENG. Under the action of the induced wind, the wind turbine rotates the shaft and rotor blades. The researchers have verified its feasibility for many self-powered wireless sensor applications such as underground tunnel lighting and billboards.

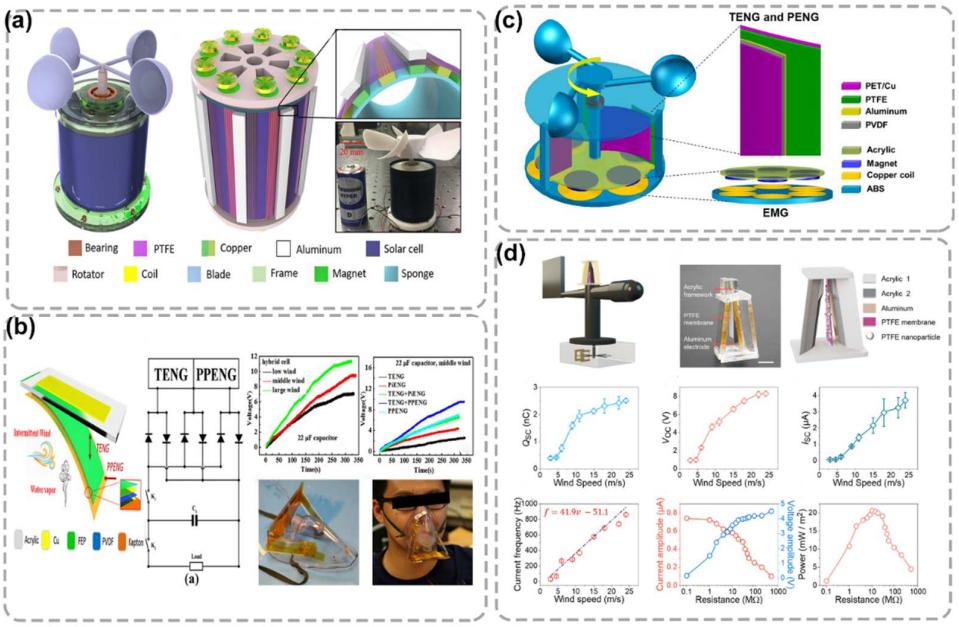

Figure 7. WD-TENG hybridized with other generators. (**a**) Hybrid TENGs combined with EMG and TENG. Reproduced with permission of [30], Copyright 2018, Elsevier. (**b**) Hybrid TENGs combined with PPENG and TENG. Reproduced with permission of [76], Copyright 2018, American Chemical Society. (**c**) Hybrid TENGs combined with PENG and TENG. Reproduced with permission of [77], Copyright 2018, Elsevier. (**d**) WD-TENG combined with photoelectric technology. Reproduced with permission of [78], Copyright 2021, Elsevier.

A TENG sensing system for simultaneous detection of wind speed and wind direction based on a rotating structure was presented in the previous paper. Although the system can achieve detection in eight directions, its multiple signal acquisition and processing ports and signal circuit design are complex. In 2022, Xu et al. designed a self-powered wind vector sensor by combining optoelectronic and triboelectric technologies [78]. As shown in Figure 7d, the sensor system consists of an angle-shaped triboelectric sensor (ASTS) at the top, a wind vane in the middle and a wind direction sensor (WDS) at the bottom. In this case, the frictional electric sensor has two disconnected Al foils attached to an acrylic plate as frictional electric layer and electrodes forming an angle of 15° between each other and a PTFE film sprayed with PTFE nanoparticles placed between them. The device based on the optimal parameters has a wide detection range in the range 2.9~24.0 m/s, within which the current frequency shows a good linear relationship with the wind speed, showing its practical potential for self-powered wind speed detection.

Now, the most common of the hybrid energy harvesting mechanisms is still the combination of TENG and EMG, where a hybrid EMG-frictional electric generator can effectively harvest broadband wind energy [79–82]. In 2021, Lu et al. designed a composite energy harvesting system consisting of a cylindrical TENG and EMG that can be used to harvest breeze energy, based on a previously studied swing-type TENG (SS-TENG) [83]. Its structure is shown in Figure 8. Its frictional electric layer has a certain air gap between it and the electrodes, and the frictional resistance is reduced, which can reduce its starting wind speed and improve the durability of the device. It can be seen that the presence of the rectifier bridge causes the output current of the EMG to drop significantly, its output

voltage itself is lower and the effective output power of the ENG is consumed to a large extent at the rectifier bridge. In the existing hybrid nano-generators, the peak and average rectified power of the TENG section are 60 and 635 times higher than the EMG section, respectively, when the coil is moderate. This result suggests that the TENG is better suited to derive energy from low frequency motion than the ENG.

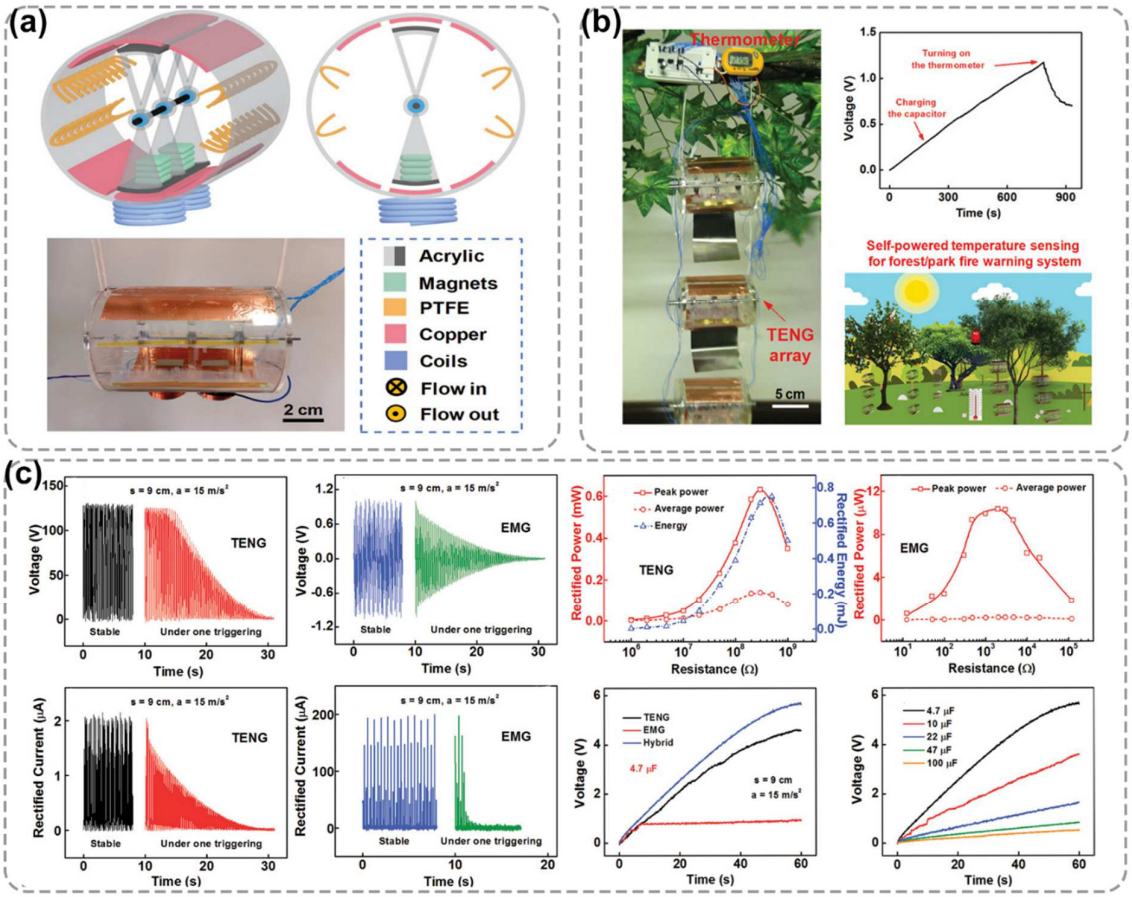

Figure 8. (**a**) A swinging breeze collection system consisting of EMG and TENG. (**b**) Photograph of a digital thermometer powered by a SS–TENG array under the wind triggering. (**c**) Output performance of the TENG part and EMG. Reproduced with permission of [83], Copyright 2021, John Wiley and Sons.

TENGs offer significant advantages in low-frequency vibration energy harvesting, but their pulse output is sparse and contact TENGs are not immune to material wear, which greatly limits their output power and stability.

In 2015, Guo et al. designed a waterproof frictional electro-magnetic hybrid generator by indirectly driving the movable part of a TENG using non-contact attraction between a pair of magnets [84]. The TENG can be driven by the attraction generated between the two sets of magnets as the EMG rotates, eliminating the need for direct contact and enabling the waterproof packaging of the TENG. The waterproof triboelectric-electromagnetic hybrid generator (WPHG) was shown to harvest wind energy and underwater water flow energy to directly power dozens of commercial LEDs during rainy days. This work has greatly facilitated the process of putting TENG and hybrid TENG into practical use. While exhibiting good output performance, these hybrid mechanism-based models tend to draw energy from only a single source and, with the limitations of power generation firmware, are difficult to package and maintain, all drawbacks that limit the use of TENGs in everyday life. In 2019, by combining EMG and TENG, Fan et al. designed a hybrid generator that converts sliding friction into a form of contact separation, where all power generating units

are completely sealed inside the equipment box and isolated from the harsh environment. Zhong et al. realized a non-contact hybrid nanogenerator (NG) with the help of a device called a magnetic coupler [85]. Experimental results show that mixed NG has higher output power than single TENG and single EMG. Because there is no physical connection between the magnetic circuit driver and the magnetic circuit, the circuit can be easily disassembled, maintained and re-installed, and the structure can easily be fully encapsulated in waterproof materials to withstand a variety of harsh environment. In 2021 the team made further optimization of the structure and proposed as shown in Figure 9b [86]. The new a multi-cylinder-based hybridized electromagnetic-triboelectric nanogenerator (MCNG) shown, which obtains dual operating frequencies through the relative rotation of two energy harvesting units, enables the harvesting of two independent fluid energies. The design provides a new idea for simultaneously harvesting independent fluid energy and improving output performance.

As exhibited in Figure 9c, Zhang et al. invented a hybrid triboelectric nanogenerator that is efficient, reliable and suitable for breeze harvesting [36]. The magnetic element not only provides the magnetic source, but also reduces the electrostatic attraction between the friction layers by its own gravity, which effectively reduces the wear of the electrode material. The design is conducive to collecting low-speed wind energy and effectively prolongs the operating life of the equipment. As shown in Figure 9d, Fan et al. designed a rotating intermittent contact TENG (IC-TENG) with automatic switching of the rotation mode [87], using a tensed rope to generate initial torsional potential energy to ensure self-activation of IC-TENG at low frequencies. This novel TENG structure provides a new strategy for low frequency vibration energy collection.

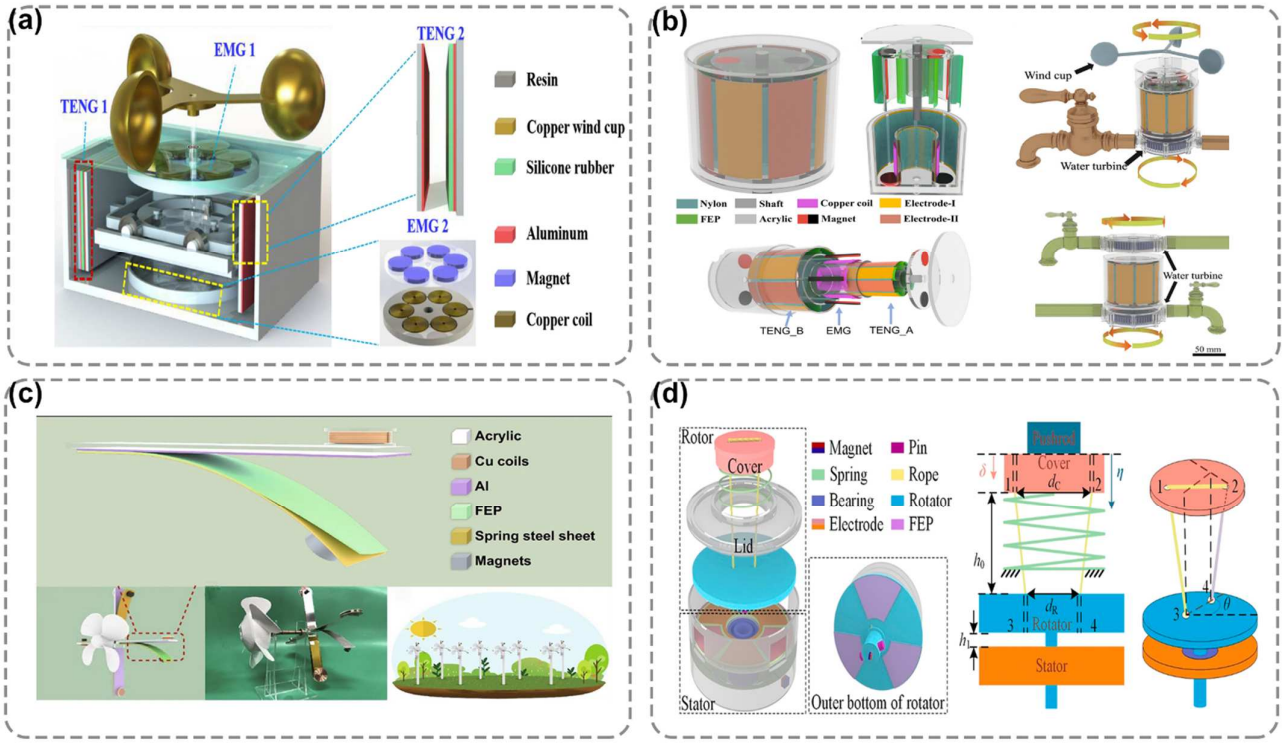

Figure 9. Hybrid TENGs combined with EMG and TENG. (**a**) The structure of the TEHG. Reproduced with permission of [88], Copyright 2019, Elsevier. (**b**) Structural design of the MCNG. Reproduced with permission of [86], Copyright 2021, Elsevier. (**c**) Schematic illustration of the W-HNG. Reproduced with permission of [36], Copyright 2020, Springer. (**d**) Structure and working principle of the IC-TENG. Reproduced with permission of [87], Copyright 2021, Elsevier.

The selection of WD-TENGs should be made in conjunction with the advantages and disadvantages of the WD-TENG classification in Table 2 and specific application

scenarios. Table 3 summarizes the reported WD-TENGs suitable for energy harvesting or sensing in breezy environments, and it is observed that wind power generation in low wind environments can be achieved by selecting flexible, low-density materials and optimizing the structure. It is expected that these more detailed presentations can provide methodological guidance and design inspiration for future research and applications of WD-TENGs in breezy environments.

Table 2. Summary and comparison of various WD-TENGs.

Structures	Triboelectric Materials	Modes	Voltage (V)	Current (uA)	Power	Ref.
Rotational sweeping mode	Al & PTFE	CS&LS	250	250	62.5 mW (900 r/min)	[29]
Rotational sweeping mode	Al & PTFE	SE	55	–	0.03 mW	[89]
Rotational sweeping mode	Al & PVDF	FT	650	50	10 mW (900 r/min)	[51]
In-plane cycled sliding mode	Cu & Kapton	FT	320	3400	–	[28]
bidirectional gear transmission structure	FEP & Cu	CS	-	-	4 mW (50 MΩ)	[23]
Transform the rotating structure into a linear structure	PTFE & Cu	CS	200	2.9	180 μw (1 subunit, 60 rpm)	[68]
Transform the rotating structure into a linear structure	PTFE & Cu	CS	320	20	0.37 mW (6 subunit, 60 rpm)	[67]
Single-side-fixed	Al & FEP	CS	100	1.6	0.16 mW (100 MΩ)	[52]
Single-side-fixed	Au & PTFE	CS	200	60	0.86 mW (15 m/s)	[58]
Single-side-fixed	FTO & PTFE	CS	36	4.1	–	[74]
Single-side-fixed	Al & PTFE	CS	400	60	3.7 mW	[54]
Single-side-fixed	FEP & Cu	CS	36	11.8	0.15 mW	[59]
Single-side-fixed	PTFE & Al	CS	297	-	0.46 Mw (10 m/s)	[26]
Single-side-fixed	Hosta Leaf & PMMA	SE	230	9.5	45 mW/m^2 (1×10^7 Ω)	[49]
Single-side-fixed	wheat straw & FEP	SE	250	20	404 μW/m^2	[48]
Single-side-fixed	PTFE & MGDY	CS	100	3.5	-	[50]
Single-side-fixed	PLL modified leaf powder & PVDF	CS	1000	60	17.9 mW (11 MΩ)	[41]
Double-side-fixed	Al & PTFE	CS	334	67	5.5 mW	[90]
Double-side-fixed	Cu &PTFE	CS	342	140	-	[53]
Lawn structure	ITO & PET	CS	78	16.3	-	[62]
Angle-shaped	FEP & Al	CS	64	2.5 (10 m/s)	-	[61]
Venturi tube	PTFE & PC	CS	-	-	4.5 mW (5 m/s)	[31]
Flag structure	Ni & Kapton	CS	40	30	135 mW/kg (22 m/s)	[32]
fluttering double-flag type	FEP & Cu	CS	-	-	600 mW/m^2 (10 m/s)	[64]
Vortex-induced	PANI & PTFE	CS	-	-	96.79 mW/m^2 (2.78 m/s)	[34]
galloping structure	Nylon & FEP	CS	200 V (1.4 m/s)	-	6 μw (1.4 m/s)	[35]
Cantilevered structure	PTFE & Al	CS	270	7.6	0.9 mw (2.9 m/s, 44 MΩ)	[33]
rolling motion of polymer beads	PTFE & Cu	FT	17.8	5.3	1.36 mW/cm^2 (20 m/s)	[66]
structure of the magnetic switch	FEP & Cu	FT	410	18	4.82 mW	[69]

Table 3. Summary and comparison of various WD-TENGs for harvest breeze wind.

Structures	Triboelectric Materials	Characteristic	Start-Up Wind Speed	Electric Output	Ref.
Rotational sweeping mode	FEP &Cu	Low density rotor material, a suitable wind scoop structure	3.3 m/s	330 v, 7 μA Pmax = 2.81 mW (4 m/s)	[56]
Rotational sweeping mode	FEP &Cu	Coupling of TENG with different structural parameters	2.2 m/s	5.2 mW	[57]
Rotational sweeping mode	FEP &Cu	Adopt the dielectric film with high flexibility	3.5 m/s	-	[91]
Vortex-induced vibration	PANI & PTFE	wind energy harvesting based on vortex-induced vibration	2.78 m/s	392.72 μW	[34]
Single-side-fixed	PTFE & Al	Controls the thickness and size of the film and the distance between the plates	3.4 m/s	297 v; 3.9 μA P = 0.46 mW (10 m/s)	[26]
Single-side-fixed	PTFE & Al	By changing the material, size and aspect ratio of the film	2.9 m/s	2.06 μW (10 MΩ)	[78]
Single-side-fixed	PTFE & MGDY	Unique material, film geometry parameter control	1.6 m/s	-	[50]
Galloping structure	Nylon & FEP	Through the design of two flexible beams to achieve galloping behavior	1 m/s	6 uW (1.4 m/s)	[35]
Cantilevered structure	Al & PTFE	Change electrode structure, electrode weight, rotating radius and cantilever length.	2.9 m/s	-	[33]
Variable diameter channel	Al & FEP	A square variable diameter channel combined with an ordinary double-ended fixed W-TENG	0.4 m/s	2 V (2 m/s)	[92]

6. Summary and Outlook

Wind energy is a widely distributed, clean, renewable and green energy source, and wind power is an important direction for future new energy development. Based on the advantages of TENG in collecting irregular low-frequency energy, WD-TENG, a new wind energy harvesting technology, is proposed to realize the effective conversion of wind energy in different applications. The existing single WD-TENG device can generate an output voltage up to 1000 V. In addition, WD-TENG can be fabricated with environmentally friend materials and the existing WD-TENG can provide power supply for low-power systems such as LEDs, temperature and humidity sensors, environmental monitor and even air cleaning device. This paper systematically reviews the evolution of WD-TENG structure, the latest progress in material selection, and compiles the output performance, advantages and disadvantages of various designs. Then, we summarize the desirable methods for WD-TENG to work effectively at different wind speeds. In addition, WD-TENG can work in concert with other mechanisms to broaden its application areas. In the future, the study of WD-TENG should devote more efforts on following areas:

1. Development of triboelectric materials

Currently, WD-TENG is often used as a self-powered wind vector sensor or to provide energy supply for small temperature and humidity sensors. The actual environmental monitoring system requires about 30–50 mW of power, and in order to ensure that the Bluetooth module continuously transmits monitoring signals to the outside world, it usually requires a large volume of TENG devices or an array of multiple devices connected in parallel. Therefore, in order to achieve a small, portable and fully self-powered environmental monitoring system, the output power density of the TENG needs to be further improved. Slip-mode WD-TENG can provide high output power, but it leads to severe material wear

and tear with frictional heat loss. Therefore, the toughness and durability of triboelectric materials are also one of the key parameters to evaluate the output performance of WD-TENG. In addition, the development of flexible, transparent, biodegradable and recyclable triboelectric materials is also an important development direction for WD-TENG to meet more application scenarios.

2. Design of the device structure

Existing device structure designs are mainly based on rotating and chattering structures. WD-TENG can reduce its start-up wind speed by reducing the weight of the device or optimizing the geometric parameters of the structure. Existing studies can achieve an average power density of 96.79 mW/m^2 at wind speeds as low as 2.78 m/s. However, new structures need to be designed to achieve the adjustment of material contact at different wind speeds, in order to maintain a universally high performance of individual devices. In addition, the establishment of mathematical models based on WD-TENG for more accurate design of energy harvesting structures and prediction of optimal operating conditions for TENG in practical applications may also become important research directions for WD-TENG in the future.

3. Power management for WD-TENG

The instability of ambient wind energy makes it difficult to transfer power directly to the load or store it by itself. Therefore, effective power management and energy storage for WD-TENGs is necessary. Existing general-purpose energy management modules for most TENGs can reduce the matching impedance of a TENG from 35 MΩ to 1 MΩ at a low frequency of 1 Hz with 80% efficiency, and can store 128 times more energy when charging a 1 mF capacitor [93]. However, these methods are not specially designed to work with wind motions. In the future, researchers need to refine and simplify the power management circuits of conventional WD-TENG, and gradually build power-managed WD-TENG to provide stable and continuous output for electronic devices.

4. Duration of WD-TENG

As already mentioned, the duration of the triboelectric material can have a great impact on the duration of WD-TENG. Besides, the external environmental conditions and with other devices also affect the durability of WD-TENG. In recent years, researchers often reduce the wear of the triboelectric layer by designing the conversion structure of non-contact working modes or by introducing lubricating substances between the contact surfaces of sliding contact TENGs. How to improve the durability of the system while maintaining high output has been a major research direction in this field.

5. Large-scale integration of WD-TENGs

The output power of existing individual WD-TENGs is not at the level of industrial applications and needs to be increased by the integration of a large number of base units. The cost of producing a single WD-TENG is not high due to the utilization of affordable thin film and simple conductive electrodes. However, the integration of a large number of TENGs inevitably brings resource consumption problems and increases the cost of power control and maintenance. Therefore, the industrialization of WD-TENG needs the joint progress of the above aspects in order to expand its application fields.

Author Contributions: X.D. prepared the review. Z.L. and P.Y. assisted in literature collation. X.C. supervised the whole process of this manuscript. All authors revised the manuscript. All authors have read and agreed to the published version of the manuscript.

Funding: This work was supported by the National Key R&D Project from Minister of Science and Technology (2021YFA1201601), the National Natural Science Foundation of China (Grant No. 62174014), Young Top-Notch Talents Program of Beijing Excellent Talents Funding (2017000021223ZK03), Beijing Nova program (Z201100006820063, Z201100006820036) and Youth Innovation Promotion Association CAS (2021165).

Conflicts of Interest: The authors declare that they have no known competing financial interests or personal relationships that could have appeared to influence the work reported in this paper.

References

1. Jain, R.K.; Qin, J.; Rajagopal, R. Data-driven planning of distributed energy resources amidst socio-technical complexities. *Nat. Energy* **2017**, *2*, 17112. [CrossRef]
2. Barrows, S.; Homer, J.; Orrell, A. Valuing wind as a distributed energy resource: A literature review. *Renew. Sustain. Energy Rev.* **2021**, *152*, 111678. [CrossRef]
3. Zhuo, Z.; Du, E.; Zhang, N.; Nielsen, C.P.; Lu, X.; Xiao, J.; Wu, J.; Kang, C. Cost increase in the electricity supply to achieve carbon neutrality in China. *Nat. Commun.* **2022**, *13*, 3172. [CrossRef]
4. Cherp, A.; Vinichenko, V.; Tosun, J.; Gordon, J.A.; Jewell, J. National growth dynamics of wind and solar power compared to the growth required for global climate targets. *Nat. Energy* **2021**, *6*, 742–754. [CrossRef]
5. Traber, T.; Kemfert, C. Gone with the wind? Electricity market prices and incentives to invest in thermal power plants under increasing wind energy supply. *Energy Econ.* **2011**, *33*, 249–256. [CrossRef]
6. Ahmed, A.; Hassan, I.; Hedaya, M.; El-Yazid, T.A.; Zu, J.; Wang, Z.L. Farms of triboelectric nanogenerators for harvesting wind energy: A potential approach towards green energy. *Nano Energy* **2017**, *36*, 21–29. [CrossRef]
7. Tummala, A.; Velamati, R.K.; Sinha, D.K.; Indraja, V.; Krishna, V.H. A review on small scale wind turbines. *Renew. Sustain. Energy Rev.* **2016**, *56*, 1351–1371. [CrossRef]
8. Gao, T.; Liao, J.; Wang, J.; Qiu, Y.; Yang, Q.; Zhang, M.; Zhao, Y.; Qin, L.; Xue, H.; Xiong, Z.; et al. Highly oriented $BaTiO_3$ film self-assembled using an interfacial strategy and its application as a flexible piezoelectric generator for wind energy harvesting. *J. Mater. Chem. A* **2015**, *3*, 9965–9971. [CrossRef]
9. Fan, F.-R.; Tian, Z.-Q.; Wang, Z.L. Flexible triboelectric generator. *Nano Energy* **2012**, *1*, 328–334. [CrossRef]
10. Wu, C.; Wang, A.; Ding, W.; Guo, H.; Wang, Z.L. Triboelectric Nanogenerator: A Foundation of the Energy for the New Era. *Adv. Energy Mater.* **2018**, *9*, 1802906. [CrossRef]
11. Wang, Z.L. Triboelectric Nanogenerators as New Energy Technology for Self-Powered Systems and as Active Mechanical and Chemical Sensors. *ACS Nano* **2013**, *7*, 9533–9557. [CrossRef] [PubMed]
12. Wang, C.; Lai, S.-K.; Wang, J.-M.; Feng, J.-J.; Ni, Y.-Q. An ultra-low-frequency, broadband and multi-stable tri-hybrid energy harvester for enabling the next-generation sustainable power. *Appl. Energy* **2021**, *291*, 116825. [CrossRef]
13. Lee, T.; Kim, I.; Kim, D. Flexible Hybrid Nanogenerator for Self-Powered Weather and Healthcare Monitoring Sensor. *Adv. Electron. Mater.* **2021**, *7*, 2100785. [CrossRef]
14. Shen, F.; Li, Z.; Guo, H.; Yang, Z.; Wu, H.; Wang, M.; Luo, J.; Xie, S.; Peng, Y.; Pu, H. Recent Advances towards Ocean Energy Harvesting and Self-Powered Applications Based on Triboelectric Nanogenerators. *Adv. Electron. Mater.* **2021**, *7*, 2100277. [CrossRef]
15. Rahman, M.T.; Rana, S.M.S.; Maharjan, P.; Salauddin; Bhatta, T.; Cho, H.; Park, C.; Park, J.Y. Ultra-robust and broadband rotary hybridized nanogenerator for self-sustained smart-farming applications. *Nano Energy* **2021**, *85*, 105974. [CrossRef]
16. Wang, Y.; Wang, J.; Xiao, X.; Wang, S.; Kien, P.T.; Dong, J.; Mi, J.; Pan, X.; Wang, H.; Xu, M. Multi-functional wind barrier based on triboelectric nanogenerator for power generation, self-powered wind speed sensing and highly efficient windshield. *Nano Energy* **2020**, *73*, 104736. [CrossRef]
17. Wang, J.; Ding, W.; Pan, L.; Wu, C.; Yu, H.; Yang, L.; Liao, R.; Wang, Z.L. Self-Powered Wind Sensor System for Detecting Wind Speed and Direction Based on a Triboelectric Nanogenerator. *ACS Nano* **2018**, *12*, 3954–3963. [CrossRef]
18. Zi, Y.; Guo, H.; Wen, Z.; Yeh, M.-H.; Hu, C.; Wang, Z.L. Harvesting Low-Frequency (<5 Hz) Irregular Mechanical Energy: A Possible Killer Application of Triboelectric Nanogenerator. *ACS Nano* **2016**, *10*, 4797–4805. [CrossRef]
19. Zhang, C.; Tang, W.; Han, C.; Fan, F.; Wang, Z.L. Theoretical Comparison, Equivalent Transformation, and Conjunction Operations of Electromagnetic Induction Generator and Triboelectric Nanogenerator for Harvesting Mechanical Energy. *Adv. Mater.* **2014**, *26*, 3580–3591. [CrossRef]
20. Bai, P.; Zhu, G.; Liu, Y.; Chen, J.; Jing, Q.; Yang, W.; Ma, J.; Zhang, G.; Wang, Z.L. Cylindrical Rotating Triboelectric Nanogenerator. *ACS Nano* **2013**, *7*, 6361–6366. [CrossRef]
21. Xi, Y.; Guo, H.; Zi, Y.; Li, X.; Wang, J.; Deng, J.; Li, S.; Hu, C.; Cao, X.; Wang, Z.L. Multifunctional TENG for Blue Energy Scavenging and Self-Powered Wind-Speed Sensor. *Adv. Energy Mater.* **2017**, *7*, 1602397. [CrossRef]
22. Lin, L.; Wang, S.; Niu, S.; Liu, C.; Xie, Y.; Wang, Z.L. Noncontact Free-Rotating Disk Triboelectric Nanogenerator as a Sustainable Energy Harvester and Self-Powered Mechanical Sensor. *ACS Appl. Mater. Interfaces* **2014**, *6*, 3031–3038. [CrossRef] [PubMed]
23. Lu, X.; Xu, Y.; Qiao, G.; Gao, Q.; Zhang, X.; Cheng, T.; Wang, Z.L. Triboelectric nanogenerator for entire stroke energy harvesting with bidirectional gear transmission. *Nano Energy* **2020**, *72*, 104726. [CrossRef]
24. He, L.; Zhang, C.; Zhang, B.; Yang, O.; Yuan, W.; Zhou, L.; Zhao, Z.; Wu, Z.; Wang, J.; Wang, Z.L. A Dual-Mode Triboelectric Nanogenerator for Wind Energy Harvesting and Self-Powered Wind Speed Monitoring. *ACS Nano* **2022**, *16*, 6244–6254. [CrossRef]
25. Phan, H.; Shin, D.-M.; Jeon, S.H.; Kang, T.Y.; Han, P.; Kim, G.H.; Kim, H.K.; Kim, K.; Hwang, Y.-H.; Hong, S.W. Aerodynamic and aeroelastic flutters driven triboelectric nanogenerators for harvesting broadband airflow energy. *Nano Energy* **2017**, *33*, 476–484. [CrossRef]

26. Xia, Y.; Tian, Y.; Zhang, L.; Ma, Z.; Dai, H.; Meng, B.; Peng, Z. An Optimized Flutter-Driven Triboelectric Nanogenerator with a Low Cut-In Wind Speed. *Micromachines* **2021**, *12*, 366. [CrossRef]
27. Ren, Z.; Wang, Z.; Wang, F.; Li, S.; Wang, Z.L. Vibration behavior and excitation mechanism of ultra-stretchable triboelectric nanogenerator for wind energy harvesting. *Extrem. Mech. Lett.* **2021**, *45*, 101285. [CrossRef]
28. Chen, S.; Gao, C.; Tang, W.; Zhu, H.; Han, Y.; Jiang, Q.; Li, T.; Cao, X.; Wang, Z. Self-powered cleaning of air pollution by wind driven triboelectric nanogenerator. *Nano Energy* **2014**, *14*, 217–225. [CrossRef]
29. Xie, Y.; Wang, S.; Lin, L.; Jing, Q.; Lin, Z.-H.; Niu, S.; Wu, Z.; Wang, Z.L. Rotary Triboelectric Nanogenerator Based on a Hybridized Mechanism for Harvesting Wind Energy. *ACS Nano* **2013**, *7*, 7119–7125. [CrossRef]
30. Qian, J.; Jing, X. Wind-driven hybridized triboelectric-electromagnetic nanogenerator and solar cell as a sustainable power unit for self-powered natural disaster monitoring sensor networks. *Nano Energy* **2018**, *52*, 78–87. [CrossRef]
31. Ravichandran, A.N.; Calmes, C.; Serres, J.R.; Ramuz, M.; Blayac, S. Compact and high performance wind actuated venturi triboelectric energy harvester. *Nano Energy* **2019**, *62*, 449–457. [CrossRef]
32. Zhao, Z.; Pu, X.; Du, C.; Li, L.; Jiang, C.; Hu, W.; Wang, Z.L. Freestanding Flag-Type Triboelectric Nanogenerator for Harvesting High-Altitude Wind Energy from Arbitrary Directions. *ACS Nano* **2016**, *10*, 1780–1787. [CrossRef]
33. Zeng, Q.; Wu, Y.; Tang, Q.; Liu, W.; Wu, J.; Zhang, Y.; Yin, G.; Yang, H.; Yuan, S.; Tan, D.; et al. A high-efficient breeze energy harvester utilizing a full-packaged triboelectric nanogenerator based on flow-induced vibration. *Nano Energy* **2020**, *70*, 104524. [CrossRef]
34. Zhang, L.; Meng, B.; Tian, Y.; Meng, X.; Lin, X.; He, Y.; Xing, C.; Dai, H.; Wang, L. Vortex-induced vibration triboelectric nanogenerator for low speed wind energy harvesting. *Nano Energy* **2022**, *95*, 107029. [CrossRef]
35. Zhang, L.; Meng, B.; Xia, Y.; Deng, Z.; Dai, H.; Hagedorn, P.; Peng, Z.; Wang, L. Galloping triboelectric nanogenerator for energy harvesting under low wind speed. *Nano Energy* **2020**, *70*, 104477. [CrossRef]
36. Zhang, Y.; Zeng, Q.; Wu, Y.; Wu, J.; Yuan, S.; Tan, D.; Hu, C.; Wang, X. An Ultra-Durable Windmill-Like Hybrid Nanogenerator for Steady and Efficient Harvesting of Low-Speed Wind Energy. *Nano-Micro Lett.* **2020**, *12*, 175. [CrossRef]
37. Lin, Z.; Zhang, B.; Guo, H.; Wu, Z.; Zou, H.; Yang, J.; Wang, Z.L. Super-robust and frequency-multiplied triboelectric nanogenerator for efficient harvesting water and wind energy. *Nano Energy* **2019**, *64*, 103908. [CrossRef]
38. Kim, D.; Tcho, I.-W.; Choi, Y.-K. Triboelectric nanogenerator based on rolling motion of beads for harvesting wind energy as active wind speed sensor. *Nano Energy* **2018**, *52*, 256–263. [CrossRef]
39. Zhu, Z.; Xiang, H.; Zeng, Y.; Zhu, J.; Cao, X.; Wang, N.; Wang, Z.L. Continuously harvesting energy from water and wind by pulsed triboelectric nanogenerator for self-powered seawater electrolysis. *Nano Energy* **2021**, *93*, 106776. [CrossRef]
40. Ren, Z.; Wang, Z.; Liu, Z.; Wang, L.; Guo, H.; Li, L.; Li, S.; Chen, X.; Tang, W.; Wang, Z.L. Energy Harvesting from Breeze Wind (0.7–6 m s^{-1}) Using Ultra-Stretchable Triboelectric Nanogenerator. *Adv. Energy Mater.* **2020**, *10*, 2001770. [CrossRef]
41. Feng, Y.; Zhang, L.; Zheng, Y.; Wang, D.; Zhou, F.; Liu, W. Leaves based triboelectric nanogenerator (TENG) and TENG tree for wind energy harvesting. *Nano Energy* **2019**, *55*, 260–268. [CrossRef]
42. Han, J.; Feng, Y.; Chen, P.; Liang, X.; Pang, H.; Jiang, T.; Wang, Z.L. Wind-Driven Soft-Contact Rotary Triboelectric Nanogenerator Based on Rabbit Fur with High Performance and Durability for Smart Farming. *Adv. Funct. Mater.* **2021**, *32*, 2108580. [CrossRef]
43. Sun, W.; Wang, N.; Li, J.; Xu, S.; Song, L.; Liu, Y.; Wang, D. Humidity-resistant triboelectric nanogenerator and its applications in wind energy harvesting and self-powered cathodic protection. *Electrochim. Acta* **2021**, *391*, 138994. [CrossRef]
44. Wang, Z.L.; Wang, A.C. On the origin of contact-electrification. *Mater. Today* **2019**, *30*, 34–51. [CrossRef]
45. Wang, D.-C.; Lei, Y.; Jiao, W.; Liu, Y.-F.; Mu, C.-H.; Jian, X. A review of helical carbon materials structure, synthesis and applications. *Rare Met.* **2020**, *40*, 3–19. [CrossRef]
46. Li, W.-S.; Sun, Y.; Hu, W.; Zhu, S.-Y.; Zhai, H.-M.; Yang, J.; Fan, X.-J.; Liu, W.-M. Tribological properties of plasma-sprayed nickel alloy matrix self-lubricating coating at elevated temperatures. *Rare Met.* **2020**, *40*, 1844–1850. [CrossRef]
47. Dudem, B.; Huynh, N.D.; Kim, W.; Kim, D.H.; Hwang, H.J.; Choi, D.; Yu, J.S. Nanopillar-array architectured PDMS-based triboelectric nanogenerator integrated with a windmill model for effective wind energy harvesting. *Nano Energy* **2017**, *42*, 269–281. [CrossRef]
48. Ma, P.; Zhu, H.; Lu, H.; Zeng, Y.; Zheng, N.; Wang, Z.L.; Cao, X. Design of biodegradable wheat-straw based triboelectric nanogenerator as self-powered sensor for wind detection. *Nano Energy* **2021**, *86*, 106032. [CrossRef]
49. Jie, Y.; Jia, X.; Zou, J.; Chen, Y.; Wang, N.; Wang, Z.L.; Cao, X. Natural Leaf Made Triboelectric Nanogenerator for Harvesting Environmental Mechanical Energy. *Adv. Energy Mater.* **2018**, *8*, 1703133. [CrossRef]
50. Li, X.; Li, Y.; Zhang, M.; Yang, Z.; Wang, K.; Huang, C. Carbon nano thorn arrays based water/cold resisted nanogenerator for wind energy harvesting and speed sensing. *Nano Energy* **2021**, *90*, 106571. [CrossRef]
51. Ren, X.; Fan, H.; Wang, C.; Ma, J.; Li, H.; Zhang, M.; Lei, S.; Wang, W. Wind energy harvester based on coaxial rotatory freestanding triboelectric nanogenerators for self-powered water splitting. *Nano Energy* **2018**, *50*, 562–570. [CrossRef]
52. Yang, Y.; Zhu, G.; Zhang, H.; Chen, J.; Zhong, X.; Lin, Z.-H.; Su, Y.; Bai, P.; Wen, X.; Wang, Z.L. Triboelectric Nanogenerator for Harvesting Wind Energy and as Self-Powered Wind Vector Sensor System. *ACS Nano* **2013**, *7*, 9461–9468. [CrossRef]
53. Wang, S.; Mu, X.; Wang, X.; Gu, A.Y.; Wang, Z.L.; Yang, Y. Elasto-Aerodynamics-Driven Triboelectric Nanogenerator for Scavenging Air-Flow Energy. *ACS Nano* **2015**, *9*, 9554–9563. [CrossRef] [PubMed]
54. Wang, S.; Mu, X.; Yang, Y.; Sun, C.; Gu, A.Y.; Wang, Z.L. Flow-Driven Triboelectric Generator for Directly Powering a Wireless Sensor Node. *Adv. Mater.* **2014**, *27*, 240–248. [CrossRef] [PubMed]

55. Li, S.; Wang, S.; Zi, Y.; Wen, Z.; Lin, L.; Zhang, G.; Wang, Z.L. Largely Improving the Robustness and Lifetime of Triboelectric Nanogenerators through Automatic Transition between Contact and Noncontact Working States. *ACS Nano* **2015**, *9*, 7479–7487. [CrossRef]
56. Li, X.; Cao, Y.; Yu, X.; Xu, Y.; Yang, Y.; Liu, S.; Cheng, T.; Wang, Z.L. Breeze-driven triboelectric nanogenerator for wind energy harvesting and application in smart agriculture. *Appl. Energy* **2021**, *306*, 117977. [CrossRef]
57. Yong, S.; Wang, J.; Yang, L.; Wang, H.; Luo, H.; Liao, R.; Wang, Z.L. Auto-Switching Self-Powered System for Efficient Broad-Band Wind Energy Harvesting Based on Dual-Rotation Shaft Triboelectric Nanogenerator. *Adv. Energy Mater.* **2021**, *11*, 2101194. [CrossRef]
58. Bae, J.; Lee, J.; Kim, S.; Ha, J.; Lee, B.-S.; Park, Y.; Choong, C.; Kim, J.-B.; Wang, Z.L.; Kim, H.-Y.; et al. Flutter-driven triboelectrification for harvesting wind energy. *Nat. Commun.* **2014**, *5*, 4929. [CrossRef]
59. Su, Y.; Xie, G.; Xie, F.; Xie, T.; Zhang, Q.; Zhang, H.; Du, H.; Du, X.; Jiang, Y. Segmented wind energy harvester based on contact-electrification and as a self-powered flow rate sensor. *Chem. Phys. Lett.* **2016**, *653*, 96–100. [CrossRef]
60. Seol, M.-L.; Woo, J.-H.; Jeon, S.-B.; Kim, D.; Park, S.-J.; Hur, J.; Choi, Y.-K. Vertically stacked thin triboelectric nanogenerator for wind energy harvesting. *Nano Energy* **2014**, *14*, 201–208. [CrossRef]
61. Lin, H.; He, M.; Jing, Q.; Yang, W.; Wang, S.; Liu, Y.; Zhang, Y.; Li, J.; Li, N.; Ma, Y.; et al. Angle-shaped triboelectric nanogenerator for harvesting environmental wind energy. *Nano Energy* **2018**, *56*, 269–276. [CrossRef]
62. Zhang, L.; Zhang, B.; Chen, J.; Jin, L.; Deng, W.; Tang, J.; Zhang, H.; Pan, H.; Zhu, M.; Yang, W.; et al. Lawn Structured Triboelectric Nanogenerators for Scavenging Sweeping Wind Energy on Rooftops. *Adv. Mater.* **2015**, *28*, 1650–1656. [CrossRef] [PubMed]
63. Wang, Y.; Yang, E.; Chen, T.; Wang, J.; Hu, Z.; Mi, J.; Pan, X.; Xu, M. A novel humidity resisting and wind direction adapting flag-type triboelectric nanogenerator for wind energy harvesting and speed sensing. *Nano Energy* **2020**, *78*, 105279. [CrossRef]
64. Sun, W.; Ding, Z.; Qin, Z.; Chu, F.; Han, Q. Wind energy harvesting based on fluttering double-flag type triboelectric nanogenerators. *Nano Energy* **2020**, *70*, 104526. [CrossRef]
65. Crusius, J.; Wanninkhof, R. Gas transfer velocities measured at low wind speed over a lake. *Limnol. Oceanogr.* **2003**, *48*, 1010–1017. [CrossRef]
66. Yong, H.; Chung, J.; Choi, D.; Jung, D.; Cho, M.; Lee, S. Highly reliable wind-rolling triboelectric nanogenerator operating in a wide wind speed range. *Sci. Rep.* **2016**, *6*, 33977. [CrossRef]
67. Gao, Q.; Li, Y.; Xie, Z.; Yang, W.; Wang, Z.; Yin, M.; Lu, X.; Cheng, T.; Wang, Z.L. Robust Triboelectric Nanogenerator with Ratchet-like Wheel-Based Design for Harvesting of Environmental Energy. *Adv. Mater. Technol.* **2019**, *5*, 1900801. [CrossRef]
68. Cheng, T.; Li, Y.; Wang, Y.-C.; Gao, Q.; Ma, T.; Wang, Z.L. Triboelectric nanogenerator by integrating a cam and a movable frame for ambient mechanical energy harvesting. *Nano Energy* **2019**, *60*, 137–143. [CrossRef]
69. Liu, S.; Li, X.; Wang, Y.; Yang, Y.; Meng, L.; Cheng, T.; Wang, Z.L. Magnetic switch structured triboelectric nanogenerator for continuous and regular harvesting of wind energy. *Nano Energy* **2021**, *83*, 105851. [CrossRef]
70. Kim, M.-S.; Tcho, I.-W.; Park, S.-J.; Choi, Y.-K. Random number generator with a chaotic wind-driven triboelectric energy harvester. *Nano Energy* **2020**, *78*, 105275. [CrossRef]
71. Xu, M.; Wang, Y.-C.; Zhang, S.L.; Ding, W.; Cheng, J.; He, X.; Zhang, P.; Wang, Z.; Pan, X.; Wang, Z.L. An aeroelastic flutter based triboelectric nanogenerator as a self-powered active wind speed sensor in harsh environment. *Extrem. Mech. Lett.* **2017**, *15*, 122–129. [CrossRef]
72. Liu, X.; Zhao, K.; Yang, Y. Effective polarization of ferroelectric materials by using a triboelectric nanogenerator to scavenge wind energy. *Nano Energy* **2018**, *53*, 622–629. [CrossRef]
73. Han, K.; Luo, J.; Feng, Y.; Lai, Q.; Bai, Y.; Tang, W.; Wang, Z.L. Wind-Driven Radial-Engine-Shaped Triboelectric Nanogenerators for Self-Powered Absorption and Degradation of NO_X. *ACS Nano* **2020**, *14*, 2751–2759. [CrossRef] [PubMed]
74. Guo, H.; Chen, J.; Tian, L.; Leng, Q.; Xi, Y.; Hu, C. Airflow-Induced Triboelectric Nanogenerator as a Self-Powered Sensor for Detecting Humidity and Airflow Rate. *ACS Appl. Mater. Interfaces* **2014**, *6*, 17184–17189. [CrossRef] [PubMed]
75. Dai, S.; Li, X.; Jiang, C.; Zhang, Q.; Peng, B.; Ping, J.; Ying, Y. Omnidirectional wind energy harvester for self-powered agro-environmental information sensing. *Nano Energy* **2021**, *91*, 106686. [CrossRef]
76. Zheng, H.; Zi, Y.; He, X.; Guo, H.; Lai, Y.-C.; Wang, J.; Zhang, S.L.; Wu, C.; Cheng, G.; Wang, Z.L. Concurrent Harvesting of Ambient Energy by Hybrid Nanogenerators for Wearable Self-Powered Systems and Active Remote Sensing. *ACS Appl. Mater. Interfaces* **2018**, *10*, 14708–14715. [CrossRef]
77. Rahman, M.T.; Salauddin; Maharjan, P.; Rasel, M.; Cho, H.; Park, J.Y. Natural wind-driven ultra-compact and highly efficient hybridized nanogenerator for self-sustained wireless environmental monitoring system. *Nano Energy* **2019**, *57*, 256–268. [CrossRef]
78. Xu, Q.; Lu, Y.; Zhao, S.; Hu, N.; Jiang, Y.; Li, H.; Wang, Y.; Gao, H.; Li, Y.; Yuan, M.; et al. A wind vector detecting system based on triboelectric and photoelectric sensors for simultaneously monitoring wind speed and direction. *Nano Energy* **2021**, *89*, 106382. [CrossRef]
79. Zhang, B.; Chen, J.; Jin, L.; Deng, W.; Zhang, L.; Zhang, H.; Zhu, M.; Yang, W.; Wang, Z.L. Rotating-Disk-Based Hybridized Electromagnetic–Triboelectric Nanogenerator for Sustainably Powering Wireless Traffic Volume Sensors. *ACS Nano* **2016**, *10*, 6241–6247. [CrossRef]
80. Cao, R.; Zhou, T.; Wang, B.; Yin, Y.; Yuan, Z.; Lin, W.Z.; Wang, Z.L. Rotating-Sleeve Triboelectric–Electromagnetic Hybrid Nanogenerator for High Efficiency of Harvesting Mechanical Energy. *ACS Nano* **2017**, *11*, 8370–8378. [CrossRef]

81. Huang, L.-B.; Xu, W.; Bai, G.; Wong, M.-C.; Yang, Z.; Hao, J. Wind energy and blue energy harvesting based on magnetic-assisted noncontact triboelectric nanogenerator. *Nano Energy* **2016**, *30*, 36–42. [CrossRef]
82. Huynh, N.D.; Lin, Z.-H.; Choi, D. Dynamic balanced hybridization of TENG and EMG via Tesla turbine for effectively harvesting broadband mechanical pressure. *Nano Energy* **2021**, *85*, 105983. [CrossRef]
83. Lu, P.; Pang, H.; Ren, J.; Feng, Y.; An, J.; Liang, X.; Jiang, T.; Wang, Z.L. Swing-Structured Triboelectric–Electromagnetic Hybridized Nanogenerator for Breeze Wind Energy Harvesting. *Adv. Mater. Technol.* **2021**, *6*, 2100496. [CrossRef]
84. Guo, H.; Wen, Z.; Zi, Y.; Yeh, M.-H.; Wang, J.; Zhu, L.; Hu, C.; Wang, Z.L. A Water-Proof Triboelectric-Electromagnetic Hybrid Generator for Energy Harvesting in Harsh Environments. *Adv. Energy Mater.* **2015**, *6*, 1501593. [CrossRef]
85. Zhong, Y.; Zhao, H.; Guo, Y.; Rui, P.; Shi, S.; Zhang, W.; Liao, Y.; Wang, P.; Wang, Z.L. An Easily Assembled Electromagnetic-Triboelectric Hybrid Nanogenerator Driven by Magnetic Coupling for Fluid Energy Harvesting and Self-Powered Flow Monitoring in a Smart Home/City. *Adv. Mater. Technol.* **2019**, *4*, 1900741. [CrossRef]
86. Zhong, Y.; Guo, Y.; Wei, X.; Rui, P.; Du, H.; Wang, P. Multi-cylinder-based hybridized electromagnetic-triboelectric nanogenerator harvesting multiple fluid energy for self-powered pipeline leakage monitoring and anticorrosion protection. *Nano Energy* **2021**, *89*, 106467. [CrossRef]
87. Fan, K.; Wei, D.; Zhang, Y.; Wang, P.; Tao, K.; Yang, R. A whirligig-inspired intermittent-contact triboelectric nanogenerator for efficient low-frequency vibration energy harvesting. *Nano Energy* **2021**, *90*, 106576. [CrossRef]
88. Fan, X.; He, J.; Mu, J.; Qian, J.; Zhang, N.; Yang, C.; Hou, X.; Geng, W.; Wang, X.; Chou, X. Triboelectric-electromagnetic hybrid nanogenerator driven by wind for self-powered wireless transmission in Internet of Things and self-powered wind speed sensor. *Nano Energy* **2019**, *68*, 104319. [CrossRef]
89. Zhang, H.; Yang, Y.; Zhong, X.; Su, Y.; Zhou, Y.; Hu, C.; Wang, Z.L. Single-Electrode-Based Rotating Triboelectric Nanogenerator for Harvesting Energy from Tires. *ACS Nano* **2013**, *8*, 680–689. [CrossRef]
90. Quan, Z.; Han, C.B.; Jiang, T.; Wang, Z.L. Robust Thin Films-Based Triboelectric Nanogenerator Arrays for Harvesting Bidirectional Wind Energy. *Adv. Energy Mater.* **2015**, *6*, 1501799. [CrossRef]
91. Wang, P.; Pan, L.; Wang, J.; Xu, M.; Dai, G.; Zou, H.; Dong, K.; Wang, Z.L. An Ultra-Low-Friction Triboelectric–Electromagnetic Hybrid Nanogenerator for Rotation Energy Harvesting and Self-Powered Wind Speed Sensor. *ACS Nano* **2018**, *12*, 9433–9440. [CrossRef] [PubMed]
92. Zhu, W.; Hu, C.; Bowen, C.R.; Wang, Z.L.; Yang, Y. Scavenging low-speed breeze wind energy using a triboelectric nanogenerator installed inside a square variable diameter channel. *Nano Energy* **2022**, *100*, 107453. [CrossRef]
93. Xi, F.; Pang, Y.; Li, W.; Jiang, T.; Zhang, L.; Guo, T.; Liu, G.; Zhang, C.; Wang, Z.L. Universal power management strategy for triboelectric nanogenerator. *Nano Energy* **2017**, *37*, 168–176. [CrossRef]